Master Thesis

Creation of 2-Dimensional Structures at the Oil-Water Interface
&
Active Particles at the Oil-Water Interface

Alice L. Townsend

Under the Supervision of:
Fuqiang Chang
Prof. dr. Willem K. Kegel

Van 't Hoff Laboratory
for Physical and Colloid Chemistry
Utrecht University
28th February 2018

Abstract

This work in Chapter 1 involves the synthesis of anisotropic colloidal particles to be used for the self-assembly of ordered 2-dimensional structures at oil-water interfaces. The particles consist of a polystyrene seed particle with a single or multiple silane oil protrusion nucleated on the polystyrene surface which are then polymerised to form an entirely solid particle. The shape and size of the protrusions grown can be tuned by silane oil concentration, base concentration and temperature. The particles synthesised are not suitable for interfacial self-assembly as the polymerisation procedure generates roughness on the particle leading to uncontrollable aggregation at the interface.

Chapter 2 involves the tracking of active particles at a bare oil-water interface and confined within a lattice structure at this interface. The active particle is a Janus particle consisting of a 5 μm polystyrene particle semi-coated in platinum. The platinum cap catalyses the decomposition of the fuel, hydrogen peroxide, and allows the particle to move via self-diffusiophoresis. The active motion of these particles was tracked and the mean squared displacement (MSD) calculated. The particles confined within a lattice saw an increased MSD and an increased velocity. This result was attributed to the steering of the active particles into a more linear track by the passive lattice particles.

Contents

1 Creation of 2D Structures of Anisotropic Colloids at an Oil-Water Interface 4
1.1 Introduction 4
1.2 Theory 5
1.2.1 Synthesis Procedure 5
1.2.2 Attractive Interfacial Forces 9
1.3 Materials and Methods 13
1.3.1 Materials 13
1.3.2 Synthesis of Polystyrene Seed Particles 13
1.3.3 Surface Modification of Seed Particles 13
1.3.4 Synthesis of Anisotropic Particles 14
1.3.5 Surface Modification of Oil Protrusion 15
1.3.6 Particle Separation 15
1.3.7 Interfacial Experiments 15
1.4 Results and Discussion 16
1.4.1 Polystyrene seed particle synthesis 16
1.4.2 Anisotropic Particle Synthesis 17
1.4.3 Polymerisation Procedure 19
1.4.4 Particle Separation 21
1.4.5 Hydrophobic Modification of TPM Protrusion 23
1.5 Conclusion and Outlook 23
2 Active Particles in 2-Dimensional Structures at the Oil-water Interface 25
2.1 Introduction 25
2.2 Theory 26
2.2.1 Active Particles 26
2.2.2 Mean Squared Displacement 27
2.2.3 Active Particles at Interface 28
2.2.4 Repulsive Interfacial Interactions 31
2.3 Materials and Methods 31
2.3.1 Materials 31
2.3.2 Polystyrene Particle Synthesis 32
2.3.3 Preparation of Janus Particles 32

2.3.4 Interfacial Experiments 33
2.3.5 Particle Position at Interface Determination 33
2.3.6 Analysis of Particle Tracking 34
2.4 Results and Discussion 34
2.4.1 Janus Particle Synthesis 34
2.4.2 Janus Particle at Oil-Water Interface 35
2.4.3 Lattice Structures at Interface 37
2.4.4 Janus Particles in Lattice Structures at Interface 37
2.4.5 Movement of Swimmer in Lattice 40
2.4.6 Particle Orientation at the Interface 41
2.5 Conclusion and Outlook 42
3 Acknowledgements 44
4 Bibliography 45
5 Appendix 48
5.1 MATLAB Codes 48
5.2 Error in Mean Squared Displacement 51

1 Creation of 2-Dimensional Structures of Anisotropic Colloids at an Oil-Water Interface

1.1 Introduction

Over one hundred years ago, Pickering[1] discovered that solid particles can spontaneously move to fluid-fluid interfaces and strongly adsorb there. Here their desorption energy can be in the range of thousands of kT[2], due to the favourable decrease in interfacial area and energy they provide. These particles in a two dimensional confinement at the interface can be subject to attractive and repulsive forces in the same manner as particles in bulk. These interactions can be manipulated and allow the particles to undergo a self-assembly at the interface.

Large particles at the interface cause deformations due to gravitational effects and when these deformations overlap create an attractive interaction between neighbouring particles. These "capillary interactions" reduce the overall interfacial area and therefore lower its overall energy. For particles on the colloidal scale, gravitational effects are not sufficient to cause deformations so some form of surface heterogeneity must be employed. These heterogeneities can arise from surface roughness, chemical heterogeneities or shape anisotropy.

Here, we focus on capillary interactions arising from the shape anisotropy of particles and how they can be manipulated to form 2-dimensional structures at an oil-water interface. The use of these capillary interactions as a way to direct anisotropic colloidal particles at the interface has been the focus of much research,[3][4] and it has been found that these colloidal particles can be directed with precise control of the orientation and the spatial arrangement. Here, we aim to synthesise anisotropic particles with a tuneable shape, and manipulate the capillary interactions at the interface to create 2-dimensional structures, such as those seen in Figure 1.1.

The synthesis procedure used involves the heterogeneous nucleation of a silane oil onto the surface of a polystyrene seed particle to form dumbbell particles or particles with multiple protrusions. We execute a surface modification and polymerization of the new protrusions grown on the polystyrene and investigate if these particles are suitable for interfacial experiments.

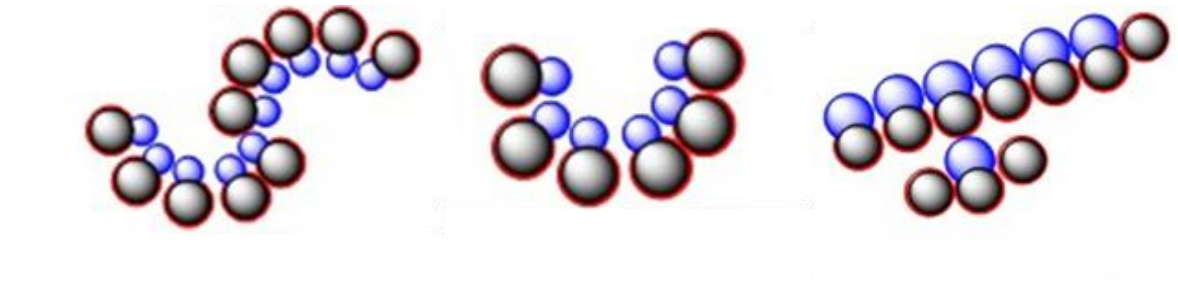

Figure 1.1: *Possible structures formed at the oil-water interface using anisotropic particles, their shape anisotropy induces capillary interactions.*

1.2 Theory

1.2.1 Synthesis Procedure

1.2.1.1 Overview of Synthesis Procedure

The synthesis of these anisotropic colloids is a method adapted from work by Sacanna et al.,[5] which employs a three step procedure. Firstly, a monodisperse solution of negatively charged polystyrene seed particles is synthesised. Following this, a hydrolysed silane oil solution is allowed to heterogeneously nucleate on the polystyrene seed surface, creating spherical protrusions. Finally, the oil-based protrusions are polymerised by means of a radical polymerisation reaction to give a fully solid composite particle. The simplified reaction scheme for this procedure is shown in Figure 1.2. This procedure should allow for full controllability over the number and size of protrusions formed on the seed particle, and produces a particle with two chemically different sites. These Janus particles formed can then undergo different chemical modification reactions on their separate entities. The core polystyrene particle can undergo surface modification to introduce halogenated groups, which will allow the particle to be further modified using click chemistry and atom transfer radical polymerisation (ATRP) reactions. The silane oil protrusion can be modified separately, for example to alter the surface wetting properties.

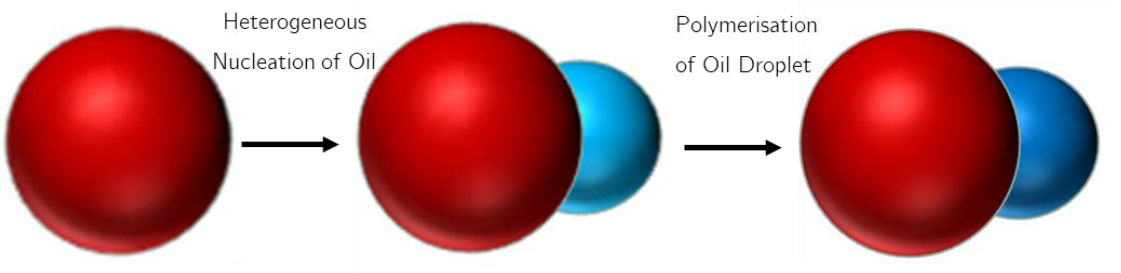

Figure 1.2: *Three step synthesis of anisotropic particles. Firstly polystyrene particles are synthesised, then oil is allowed to heterogeneously nucleate on the polystyrene particles before being polymerised to a solid protrusion.*

1.2.1.2 Formation of New Protrusion

The most common procedure to synthesise anisotropic particles from spherical seeds is by way of an internal phase separation. The general procedure involves the swelling of a seed particle with excess monomer, allowing elastic stress to build up in the particle. This stress is relieved by the phase separation of some monomers from the seed particle, during a heating stage, creating a new protrusion, as first reported by Sheu *et al.*[6] This technique may not allow for separate modification of the seed particle and protrusion or for separate polymerisation of each section of the particle.

The method employed in this research, of nucleating an oil droplet on the surface of the seed particle, can be a more controllable technique. This method allows for the formation of two

chemically different regions which can be controlled in their size and shape. This system also allows for selective polymerisation of each lobe, adding another degree of freedom in this method.

There are three main steps for the formation of a new protrusion on the seed particle: hydrolysis, condensation and polymerisation. Firstly, the oil monomers must be hydrolysed to water-soluble silanols. The oil utilised here is 3-methacryloxypropyl trimethoxysilane (TPM) as it possesses hydrolysable alkoxy silane groups. TPM is slowly hydrolysed in water with vigorous stirring, see Figure 1.3, a relatively slow procedure at neutral pH.[7]

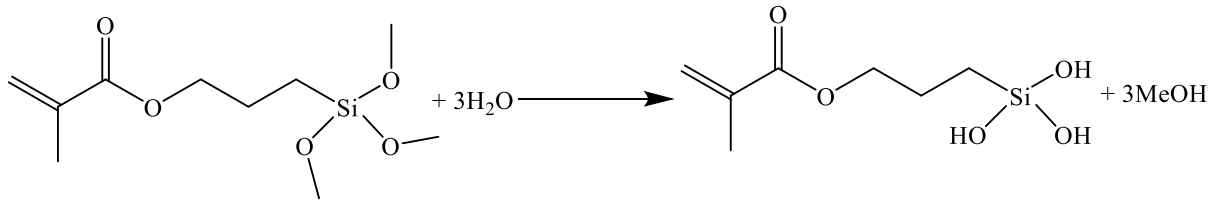

***Figure 1.3**: Reaction scheme for the hydrolysis of TPM to form water-soluble silanols.*

The hydrolysed TPM monomers then undergo a base-catalysed condensation to form branched silsesquioxanes, which are no longer water-soluble once they reach their equilibrium solubility,[8] depicted in Figure 1.4. If no seed particles are present, free oil droplets will form.[9] Above pH 9 TPM monomers are negatively charged, allowing for a negative surface charge on the oil droplet,[8] which prevents these droplets from coalescing. The oil droplets size can be tuned by monomer addition and concentration of base added.[9] If seed particles are present, these oil droplets will heterogeneously nucleate on the surface of the seed, creating either an engulfing layer or a spherical protrusion depending on the wettability of the seed particle. In general, a positively charged seed particle will be fully engulfed in an oil droplet, whereas a negatively charged particle sits at the oil-water interface, leaving a section of the seed particle exposed.[5] The polystyrene particles used in this report have a negative charge allowing for oil droplets to nucleate on the particles surface without fully surrounding the seed particle.

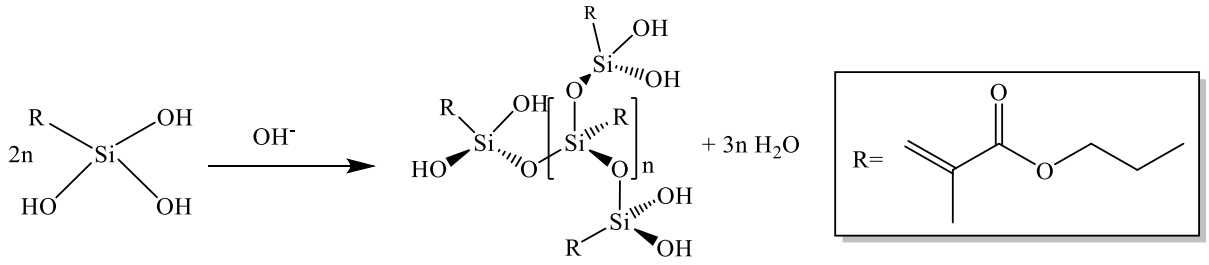

***Figure 1.4:** Reaction scheme for base catalysed condensation of TPM silanols to form branched silsesquioxanes.*

1.2.1.3 Polymerisation of Oil Protrusion

At this stage, the TPM protrusion is still liquid and needs to be solidified to get a stable composite particle. In order to achieve this, a free-radical polymerisation technique is used. The oil-soluble radical initiator azobisisobutyronitrile (AIBN) is heated to the polymerization temperature

(70 °C) and decomposes to form two cyanoprop-2-yl radicals and nitrogen gas, shown in Figure 1.5. The radicals then attack the methacrylate moiety of the TPM which allows for polymerisation due to the reactive nature of the double bond. As AIBN is an oil soluble initiator, it can enter the oil droplet and allow for polymerisation from the inside, preserving its surface structure. The particles can then be washed in ethanol without loss of the newly formed protrusion.

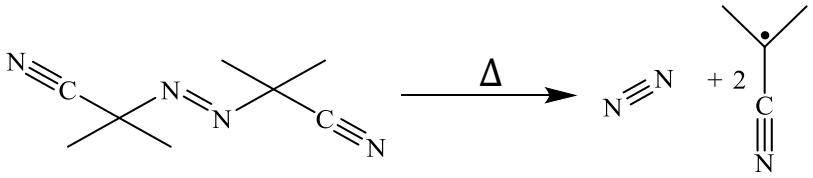

***Figure 1.5**: Thermal decomposition of free radical initiator AIBN into nitrogen gas and 2 cyanoprop-2-yl radicals.*

By the end of this synthesis method we should have produced monodisperse particles with one or more chemical different protrusions that are solid and stable. These particles should be stable at the interface and only aggregate due to capillary interactions, as described below.

1.2.1.4 Hydrophobic Modification

In order to increase the stability of the oil protrusion at the interface, a surface modification is employed. Hexamethyldisilazane is used to cap the surface silanol groups of the TPM with bulky trimethoxysilane groups in order to induce hydrophobicity, the reaction scheme of which is show in Figure 1.6.

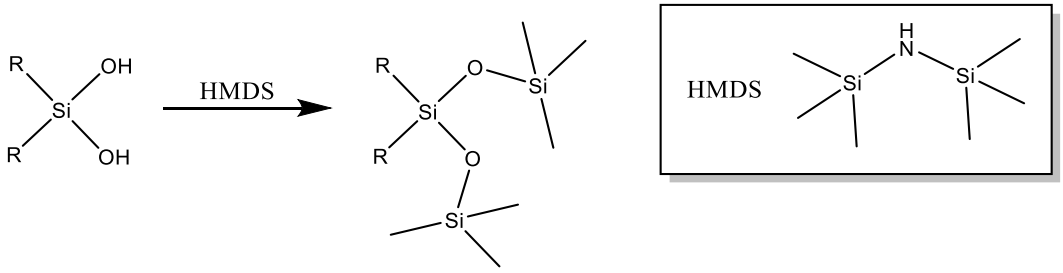

***Figure 1.6**: Hydrophobic modification procedure of capping the silanol surface groups of the TPM protrusion with trimethoxysilane groups from hexamethyldisilazane.*

Previous results show that the hydrophobic modification procedure is necessary for the silane lobe to be stable at the interface. Figure 1.7 shows polystyrene particles with a 3-(Trimethoxysilyl)propyl acrylate (TMSPA) shell at an oil-water interface. TMSPA has a very similar structure to TPM so they can be compared easily. In Figure 1.7A the PS-TMSPA core-shell particles are unstable at the interface and form aggregates. Figure 1.7B shows the particles at the interface after they have been modified hydrophobically, and the more stable, well-spaced structure they form.

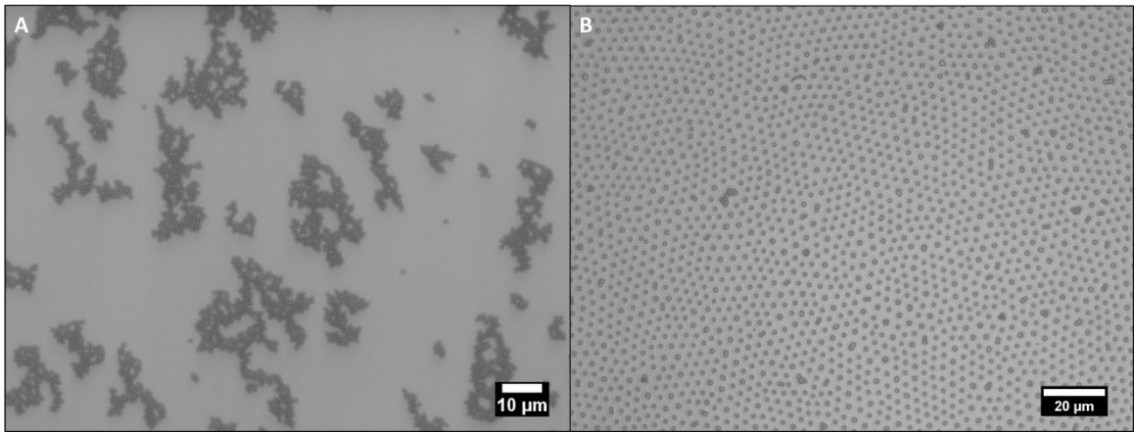

***Figure 1.7**: TMSPA-PS core-shell particles at the oil-water interface with (a) no surface modification (b) hydrophobic surface modification.*

The stability can be explained by the contact angle of the particle at the interface. For an interfacial particle this can be referred to as the three phase contact angle (ϑ). It is defined as the angle between the solid particle and the interface measured through either liquid phase, here we take the angle through the water phase as shown in Figure 1.8. This contact angle is dependent on the interfacial tensions between the particle and water (γ_{pw}), the particle and oil (γ_{po}) and between the water and oil (γ_{ow}), via Young's Equation:

$$Cos\ \theta = \frac{\gamma_{po} - \gamma_{pw}}{\gamma_{ow}} \qquad (1.1)$$

The wettability of the particle can alter the contact angle. For particles with an equal wettability in each phase, the contact angle will be 90°. The angle will increase for more hydrophobic particles and decrease for hydrophilic particles.

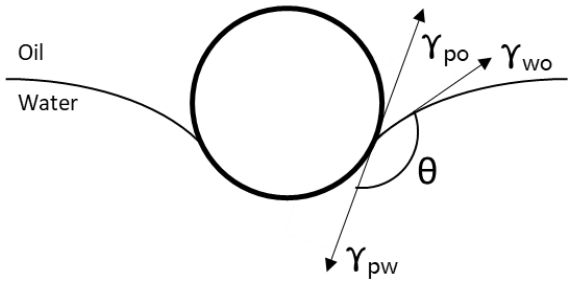

***Figure 1.8**: The three phase contact angle (θ) of a heavy solid particle at an oil-water interface, showing the three interfacial tensions between the particle, water and oil.*

The repulsive forces that keep the particles stable at the interface can be attributed to Coulombic repulsion through the oil phase of the like-charged particles. The fraction of the particle's surface in the oil-phase needs to be large enough to allow for significant Coulomb repulsion.[10] The effect of the particles contact angle to the interface is shown in Figure 1.9, for hydrophilic silica

particles with a contact angle less than 90° disordered, aggregated structures are formed, for more hydrophobic particles with larger contact angles well-ordered structures are seen.[11]

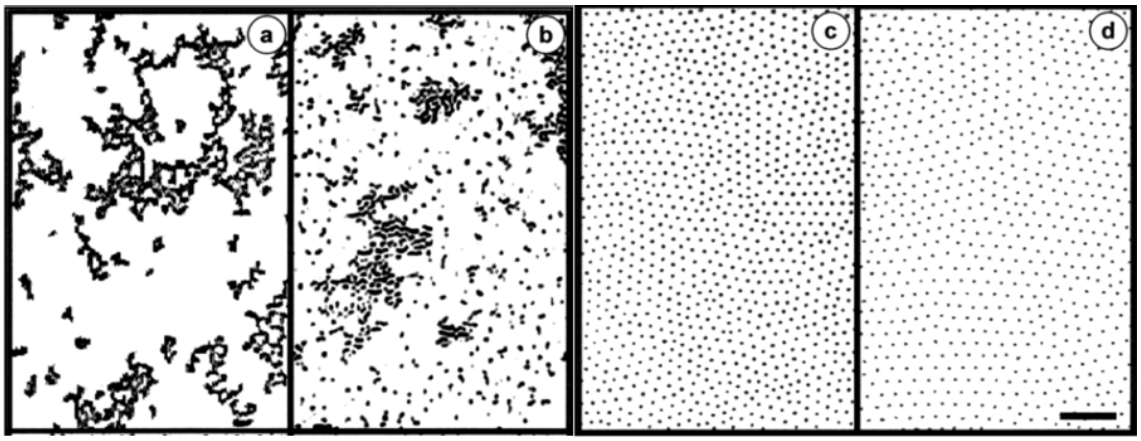

***Figure 1.9**: Monolayers of silica particles at oil-water interface with contact angles of (a) 70° (b) 115° (c) 129° (d) 150°. From figure 1 in [11].*

1.2.2 Attractive Interfacial Forces

The aim of this project is to create tuneable 2-dimensional structures at an oil-water interface by manipulating capillary interactions of the particles. Trapping particles at an interface is favourable energetically as it lowers the surface area of the interface and thus its overall energy. Due to this, the step of introducing particles to the interface is a simple one. Once the particles are at the interface, the attractive forces working on the particles will be controlled and utilised in the self-assembly procedure.

Van der Waal Forces

The simplest attractive forces working on the particles at the interface are van der Waals interactions. If sufficient salt is present in either liquid phase to screen the stabilising electrostatic effects of the charged colloids, aggregation via van der Waals forces can occur. The energy of the van der Waals interactions can be notified as such:

$$E_{vdw} = \frac{AR}{12D} \qquad (1.2)$$

Where A is the Hamaker constant, R is the particle radius and D the distance between the particle surfaces. However, if D exceeds 1 μm, E_{vdw} will be much smaller than the thermal energy k_BT.[12] Therefore, as particles at oil-water interfaces are generally separated by distances larger than their radaii, the Van der Waals interactions are not significant here.

Capillary Interactions

As van der Waals interactions have been discounted there must be another force at play which induces the aggregation of particles at an interface. Attractive forces between particles can arise when the interface is deformed by particles and a larger interfacial surface area created, which

leads to an unfavourable increase in interfacial energy. To counteract this energy increase, deformations of neighbouring particles will overlap, form a single deformation and pull the particles closer together. These interactions are described as lateral capillary interactions. For particles on the macroscale, these interfacial deformations are caused by gravitational interactions, depicted in Figure 1.10 (a). If the menisci of the deformations have the same sign, i.e. both point upwards or downwards, the particles will attract. If the menisci have opposite signs, the particles can repel, as seen in Figure 1.11 (a). These types of capillary interactions are called "floatation forces" and due to the force of these interactions decreasing with R^6, for a particle of radius less than 10 μm these forces are non-existent.[13]

For smaller particles, which are not heavy enough to create local deformations on the interface, capillary interactions are still evident. These attractions can be referred to as "immersion forces",[13] shown in Figure 1.10 (b), and arise from the position of the contact line and the contact angle of the particle at the interface.

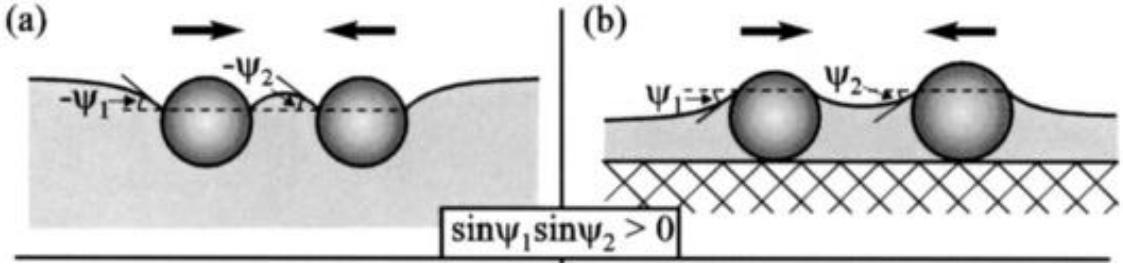

Figure 1.10*: (a) showing capillary interactions formed from gravitational deformations of the interface (b) capillary interactions from immersion forces at the interface. From figure 1 in [13].*

If the small particles are fully smooth chemically heterogeneous spheres, no attraction between the particles is seen, shown in Figure 1.11 (b), due to the fact that the contact line at the interface is completely straight.[14] If the particles have any surface roughness, chemical heterogeneity or shape anisotropy, capillary interactions can be induced.

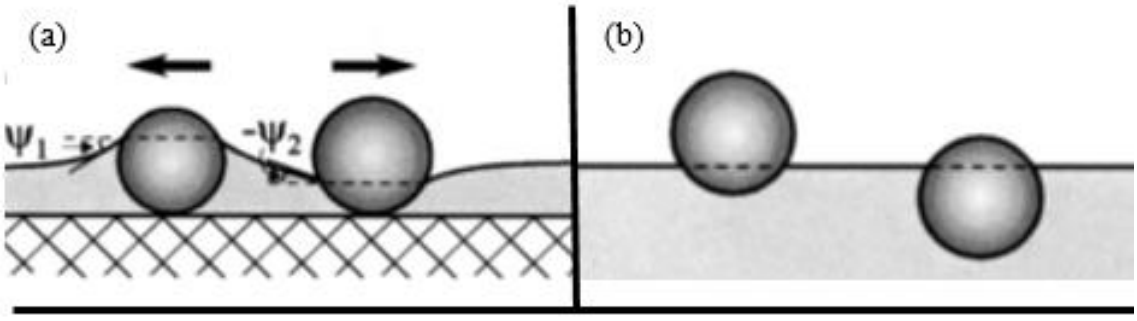

Figure 1.11*: (a) the repulsion of a hydrophilic and a hydrophobic particle at the interface due to opposite menisci (b) particles which cause no deformations at the interface will have no capillary interactions between them. Adapted from Figure 1 in [13].*

The surface roughness of a particle creates an undulated contact line at the interface, shown in Figure 1.12, inducing strong aggregation of these particles. The contact line pins strongly to the heterogeneities on the particles surface (roughness) creating the interfacial deformations which induce capillary forces. Even undulations of the interface on the nanoscale can induce capillary interactions, with the interaction energy being in the order of 10^4 *kT*.[15]

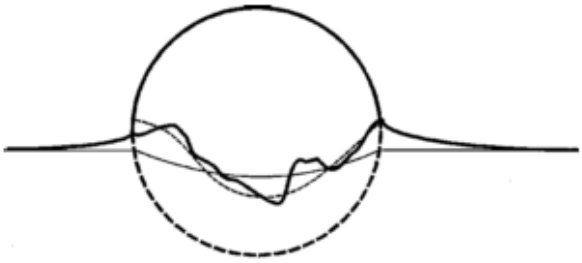

Figure 1.12*: The contact line at the oil-water interface is ideally straight to prevent capillary interactions but if surface heterogeneities are present this line can pin to them and become undulated. Adapted from Figure 1 in [12].*

For particles that posess some type of chemical heterogeneity, capillary interactions can be induced. For example, particles with a hydrophilic and a hydrophobic region have non-uniform wetting at the interface, leading to an irregular contact line and thus attractive interactions between the particles.

The final property which can induce capillary interactions at the interface is shape anisotropy. Particles with a more complex shape than spheres can create undulations in the contact line of the interface and induce attractive forces. As evidenced by Loudet *et al.* [3] during their work on anisotropic ellipsodial particles, anisotropic particles at the interface can create strong capillary interactions due to their more complex interfacial distortions. For polystyrene based ellipsoids, they form chain-like structures at the interface, shown in Figure 1.13. These structures form as a larger interfacial deformation is created at the tip of the ellipsoid due to its sharp point, thus inducing capillary interactions at this position.

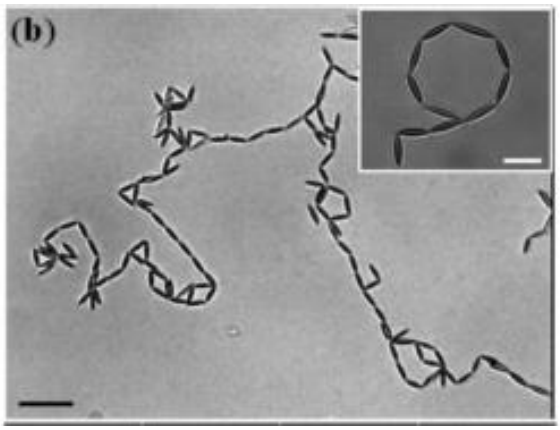

***Figure 1.13**: Chain-like structures formed by ellipsoidal polystyrene particles at an oil-water interface due to capillary interactions. Adapted from Figure 1 in [3].*

From previous work completed in this research group we can predict the structures that the dumbbell shaped particles we synthesise will form. At the junction between the lobes of the particle a sharper angle is present, indicated by the arrows in Figure 1.14, and we expect a larger interfacial deformation at these points. Here a quadrupole-like interaction is expected as seen with ellipsoidal particles[3].

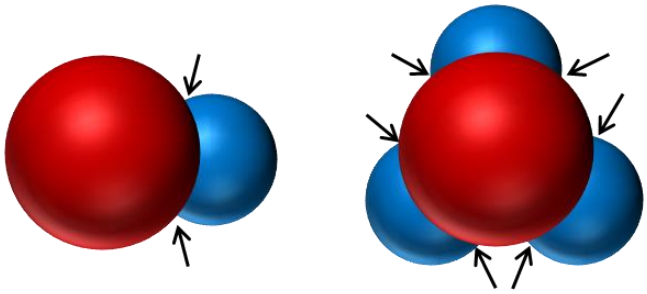

***Figure 1.14**: Expected structures of anisotropic particles with arrows showing the points at which larger interfacial deformations are formed due to the sharp angle of curvature at these points.*

Due to these deformations we expect dumbbell particles to line up side by side as shown in Figure 1.15 B,C. By changing the protrusion size we expect to be able to change the curvature of the chains, as shown in Figure 1.15 E,F. By changing the chemical properties of each protrusion we should be able to manipulate the structure further, with the linking of multiple chains for example. By altering the shape of the particle, by adding more protrusions for example, more complex structures should form at the interface due to capillary interactions.

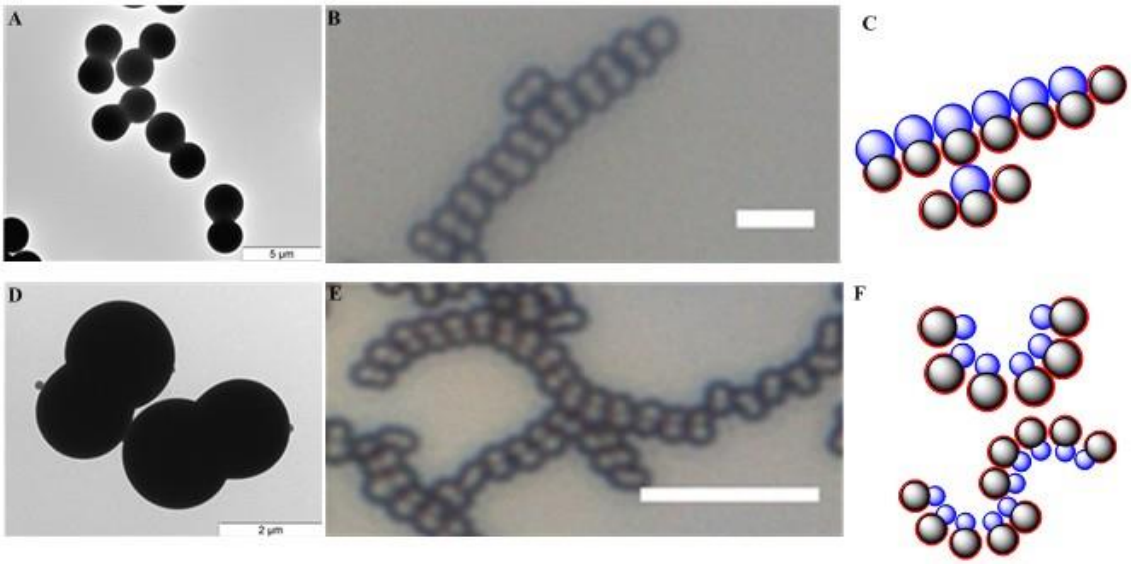

Figure 1.15: *A,D: SEM images of dumbbell shaped particles with differing size ratios. B,E: Optical microscopy images of the structures of these particles formed by capillary interactions. C,F: Simplified diagrams of the structures formed. Image: Fuqiang Chang.*

1.3 Materials and Methods

1.3.1 Materials

Chemical	Source
2,2′-Azobis(2-methylpropionitrile)	Fisher Scientific
Styrene (≥99%)	Sigma-Aldrich
Methanol (≥99%)	Biosolve
4-Styrenesulfonic acid sodium salt hydrate (Mw=206.19)	Aldrich
Divinylbenzene (80%)	Aldrich
2-(2-Bromoisobutyryloxy)ethyl methacrylate	Sigma-Aldrich
Ethanol (ACS ISO reagent)	Emsure
3-(Trimethoxysilyl)propyl methacrylate (98%)	Sigma-Aldrich
Ammonia (28-30 wt.%)	Fisher Scientific
Hexamethydisilazane (99%)	Sigma-Aldrich
Potassium iodide	VWR Internaional BV
Ficoll® PM 400	Sigma-Aldrich
Decane (≥99%)	Sigma-Aldrich

All water used has been filtered through a MilliQ® water purification system. Decane was purified by removing the polar components by adsorption onto aluminium oxide powder.[16] All other chemicals were used without further purification.

1.3.2 Synthesis of Polystyrene Seed Particles

The procedure used for the preparation of 1.5 μm polystyrene particles is as follows: 90 mg 2,2′-Azobis(2-methylpropionitrile) (AIBN), 8 mL styrene and 40 mL methanol were added to a 100 mL round bottom flask. 130 mg 4-Styrenesulfonic acid sodium salt hydrate (NaSS) was dissolved in 10 mL milliQ water and added to the flask. The reaction vessel was degassed under nitrogen for 30 minutes with continuous stirring, then heated to 80°C in an oil bath to initiate the reaction. After 2.5 hours of heating a second batch of chemicals was added to increase the particle size. 10 mL methanol, 30 μL divinylbenzene (DVB) and 2 mL styrene were combined and then added to the flask. The reaction was left to run for 20 hours. Once reaction was complete flask was removed from oil bath to quench the reaction and the solution was transferred to a 100 mL centrifuge tube. The solution was washed at 2000 rpm for 30 minutes with milliQ water 3 times.

1.3.3 Surface Modification of Seed Particles

A surface modification procedure was carried out on the polystyrene seed particles to introduce brominated surface groups, which can allow for further modification of the seed lobe. 2 mL 18

wt.% polystyrene seed solution was placed in a 40 mL vial with 10 mL milliQ water and ultrasonicated for 30 minutes to break up any aggregates. 3.5 mg AIBN was dissolved in an oil phase consisting of 72 µL 2-(2-Bromoisobutyryloxy)ethyl methacrylate (BIEM) and 288 µL styrene. The oil phase was added to the polystyrene solution and left on a roller table at 60 rpm for 12 hours before being transferred to a 70 °C oil bath for polymerisation to occur. The sample was left in the oil bath for 12 hours with constant stirring. The solution was then placed in a centrifuge tube with milliQ water and centrifuged at 1200 rpm for 10 minutes. This washing procedure was repeated 3 times.

1.3.4 Synthesis of Anisotropic Particles

To prepare snowman particles consisting of a polystyrene seed and an oil based protrusion the following method was used: to prepare the 3-(Trimethoxysilyl)propyl methacrylate (TPM) oil solution, 1 mL of TPM oil was hydrolyzed in 10 mL milliQ water with vigorous stirring for 6 hours. The reaction is completed when the resulting solution is fully clear and free from oil droplets. The hydrolyzed TPM solution was stored in the freezer at -20 °C in 1 mL vials to prevent degradation.

To prepare snowman particles, 0.5 mL 0.3 wt.% brominated polystyrene seed solution was combined with varying amounts of TPM solution and fresh ammonia (1 µL/mL) solution in a 4 mL vial. The ammonia solution was prepared by diluting 10 µL 28% ammonia with 10 mL milliQ water. The vial was left on a roller table at 10 rpm for 15 hours.

To polymerise the TPM lobe formed in this experiment, a few different polymerization procedures were utilised. These procedures are all for samples in which 200 µL of TPM solution was added, so the ratio of AIBN/TPM is 1 mg/50 µL.

For the first polymerization method, 4 mg of AIBN salt was added to the reaction vial and placed in a 90 °C oven for 2 hours in order for the AIBN salt to dissolve. The sample was then transferred to a 70°C oil bath for 12 hours, with stirring. The resulting solution was transferred to a centrifuge tube and washed with ethanol at 3500 rpm for 1 minute, this step was repeated 3 times.

In the next procedure, 100 µL of 1 µL/mL ammonia in milliQ water solution was added to the reaction vial to induce the nucleation of all TPM monomers left in the solution. A 2,2′-Azobis(2-methylpropionitrile) solution was prepared by adding 15 mg of AIBN to 1 mL methanol and allowing the AIBN to dissolve. 300 µL of this AIBN solution was added to the reaction vial and the vial transferred to a 70°C oil bath for 12 hours, with stirring. The resulting solution was washed as above.

The third procedure involved the reaction vial being left in an 85 °C oven for 3 hours before 4mg AIBN were added to the reaction vial and it was placed in a 70°C oil bath for 12 hours, with stirring. The particles were washed as above.

The final polymerization method used is as follows: to prepare the AIBN solution 3mg AIBN was dissolved in 50 µL of TPM oil and this solution was then added to the reaction vial of snowman particles. The sample was left on the roller table for 2 hours at 60 rpm before being transferred to a 70°C oil bath for 12 hours, with stirring. The washing procedure for the particles is as above.

1.3.5 Surface Modification of Oil Protrusion

In order for the oil protrusions to be stable at the oil-water interface, a surface modification to induce hydrophobicity is needed. 0.5 mL 0.3 wt.% snowman particle in ethanol solution was added to a 4 mL glass vial. 6 mg potassium iodide dissolved in 30 µL hexamethyldisilazane (HMDS) was added to the vial and the solution left on the roller table at 60 rpm for 24 hours.

To test the hydrophobic modification procedure it was first carried out on TPM sphere. The procedure was as follows: 1mL 10uL/mL ammonia solution was added to 2.5 mL hydrolysed TPM solution (solution turns cloudy immediately) and left on the roller table at 10 rpm for 3 hours. To polymerise the spheres, 50 µL AIBN solution was added (3mg/50uL TPM oil) and left on roller table at 10 rpm for 2 hours before being transferred to 70°C oil bath for 18 hours. The particles were washed in milliQ water once and ethanol 3 times.

1.3.6 Particle Separation

To separate the particles to get pure sample of each particle structure, density gradient centrifugation was used. A 30 mL continuous gradient of 8-20 wt.% ficoll was prepared in a centrifuge tube and 300 µL 0.4 wt.% sample was added on top of the ficoll, the set up shown in Figure 1.16. The sample was then centrifuged at 800 rpm for 15 minutes leading to the appearance of bands in the solution. Each band was removed separately from the sample using a syringe and washed with milliQ water at 2500 rpm for 45 seconds 5 times.

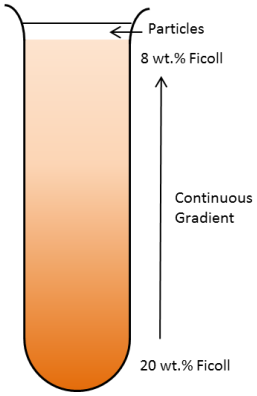

***Figure 1.16**: Density gradient centrifugation centrifuge tube, with a continuous gradient of 8-20 wt.% Ficoll.*

1.3.7 Interfacial Experiments

A fluid cell was used to create a flat and stable oil-water interface. The fluid cell consists of a glass base with a glass outer ring in the centre. Outside of the outer ring the base has a thickness of 1 mm to allow for mounting of the cell on a microscope, and inside the glass ring the base thickness is 150 µm to allow for clear imaging of the interface. The outer glass ring houses an inner ring consisting of an aluminium ring with a Teflon insert. The aluminium ring has four large spacers in its base to allow for the flow of liquid between the inner and outer rings. The entire glass ring

is covered by a glass cap to protect the sample and prevent evaporation. The fluid cell structure is shown in Figure 1.17.

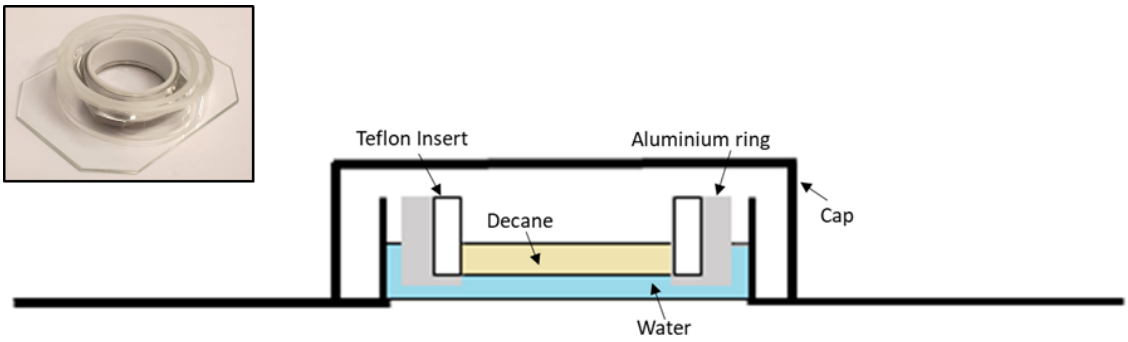

Figure 1.17: *Fluid cell components, inset is image of fluid cell.*

To prepare an oil-water interface, 1.6 mL of an aqueous phase was transferred to the cell followed by 0.6 mL of purified decane slowly added on top of the aqueous phase. The colloidal suspension of interest, dispersed in ethanol, was injected using a syringe slightly below the decane-water interface but above the glass base. This allowed the particles to move up to the interface and become pinned there and prevented them sticking to the glass base.

A motorised Nikon Ti Eclipse inverted optical microscope was used to image the interface, with a Nikon 60x air objective with a working distance of 1.3 mm. The microscope is controlled by NIS Elements software and images of an .nd2 format were recorded.

1.4 Results and Discussion

1.4.1 Polystyrene seed particle synthesis

The method of preparation of polystyrene spheres is a successful and easily reproducible one. The procedure above produces a solution of monodisperse negatively charged polystyrene particles with a radius of approximately 1.5 μm. An optical microscopy image of these polystyrene particles is shown in Figure 1.18.

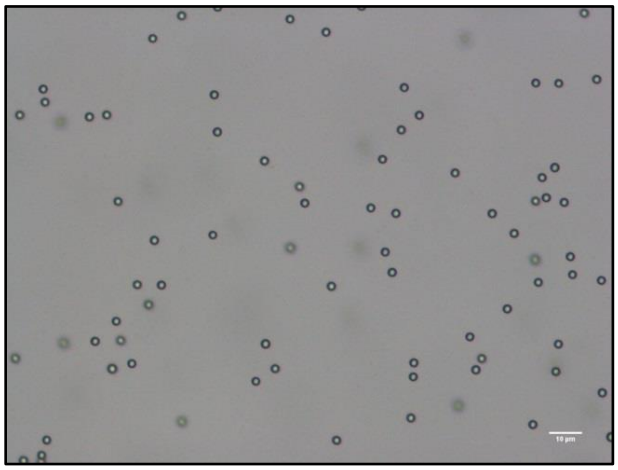

***Figure 1.18**: Optical microscopy image of 1.5 µm polystyrene particles in milliQ water.*

1.4.2 Anisotropic Particle Synthesis

The procedure used above is one which can be modified to produce particles with different size protrusions and a different number of protrusions. Many conditions can alter the structure of the particles produced so it can be difficult to control this procedure. Temperature, base concentration and TPM monomer concentration can affect the growth procedure. All the samples referred to in this results section consist of a mixture of different shape particles, polystyrene spheres and free TPM spheres.

Effect of TPM Concentration

The concentration of TPM used in the experiment can alter the size of the protrusions formed. Sample I, shown in Figure 1.19, prepared with the lowest concentration of TPM, displays a single, small protrusion on each polystyrene seed particle. If the concentration of TPM is increased, the protrusion size is also increased. Sample II and sample III have increasing concentrations of TPM and show increasing size of the protrusion. This agrees with the findings of Sacanna *et al*. [9] that the size of TPM spheres can be increased by increasing monomer concentration.

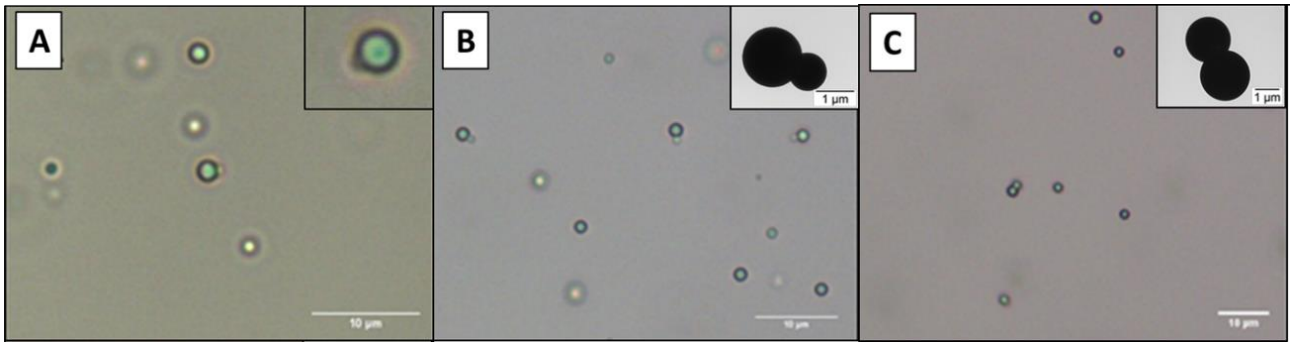

***Figure 1.19**: Optical microscopy and SEM (inset) images of dumbbell particles (a) Sample I (b) Sample II and (c) Sample III.*

Table 1

Sample	TPM	MilliQ water	Polystyrene (0.3 wt.%)	Ammonia Solution (1 µL/mL)
I	50 µL	1 mL	0.5 mL	15 µL
II	200 µL	1 mL	0.5 mL	15 µL
III	250 µL	1 mL	0.5 mL	15 µL

Effect of Base Concentration

The concentration of base used in this procedure can affect the number and size of the TPM protrusions formed. Figure 1.20 illustrates this effect. For sample I a low concentration of base was used, the particles have multiple protrusions which are very small. As the concentration of

base is increased the protrusions grow in size, reaching an approximately 1:1 size ratio with the seed lobe for the highest concentration of ammonia used, shown in Figure 1.20 C.

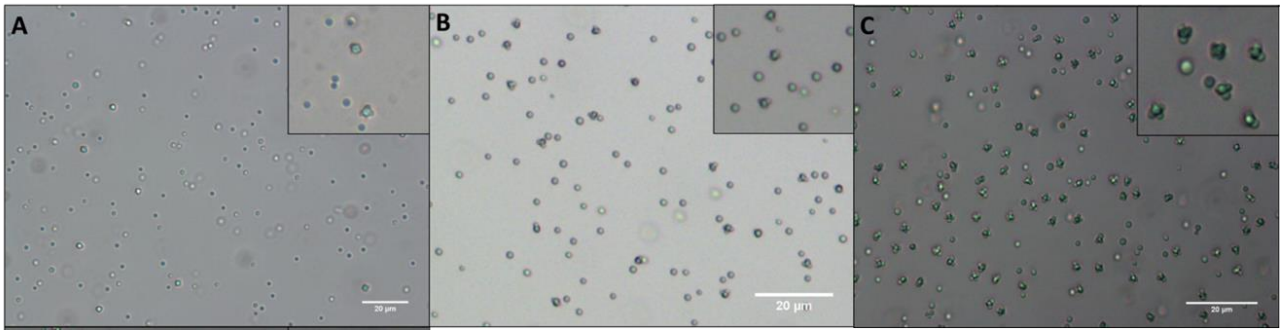

Figure 1.20*: Optical microscopy images of the effects of base concentration on the synthesis procedure on (a) sample I, (b) sample II and (c) sample III.*

Table 2

Sample	TPM	MilliQ water	Polystyrene (0.3 wt.%)	Ammonia Solution (1 µL/mL)
I	200 µL	1 mL	0.5 mL	5 µL
II	200 µL	1 mL	0.5 mL	10 µL
III	200 µL	1 mL	0.5 mL	40 µL

Temperature Effects

The temperature at which the experiment is carried out can affect the structure of the particles formed, in particular the number of protrusions which form on the seed particle. For experiments carried out at 3 °C, the reaction vial was placed in a fridge and shaken gently every 30 minutes. Under these conditions, only one or two protrusions form on the seed particles, shown in Figure 1.21 A. For experiments carried out at room temperature, approximately 18 °C, particles with two or three protrusions are seen with the protrusion size increased than that of the procedure at 3 °C, shown in Figure 1.21 B. If the reaction is carried out in a 50 °C oven, with gentle shaking every 30 minutes, particles generally have three or four protrusions, seen in Figure 1.21 C. This temperature effect can be attributed to the fact that extra energy is being added to the system allowing for more TPM monomers to nucleate on the seed particle. This trend does not continue for higher temperatures. For a sample with the procedure carried out in an 85 °C oil bath there is no trend for the number of protrusions on the particle. In Figure 1.21 D, particles with two, three and four protrusions are evident with no overwhelming majority of one structure.

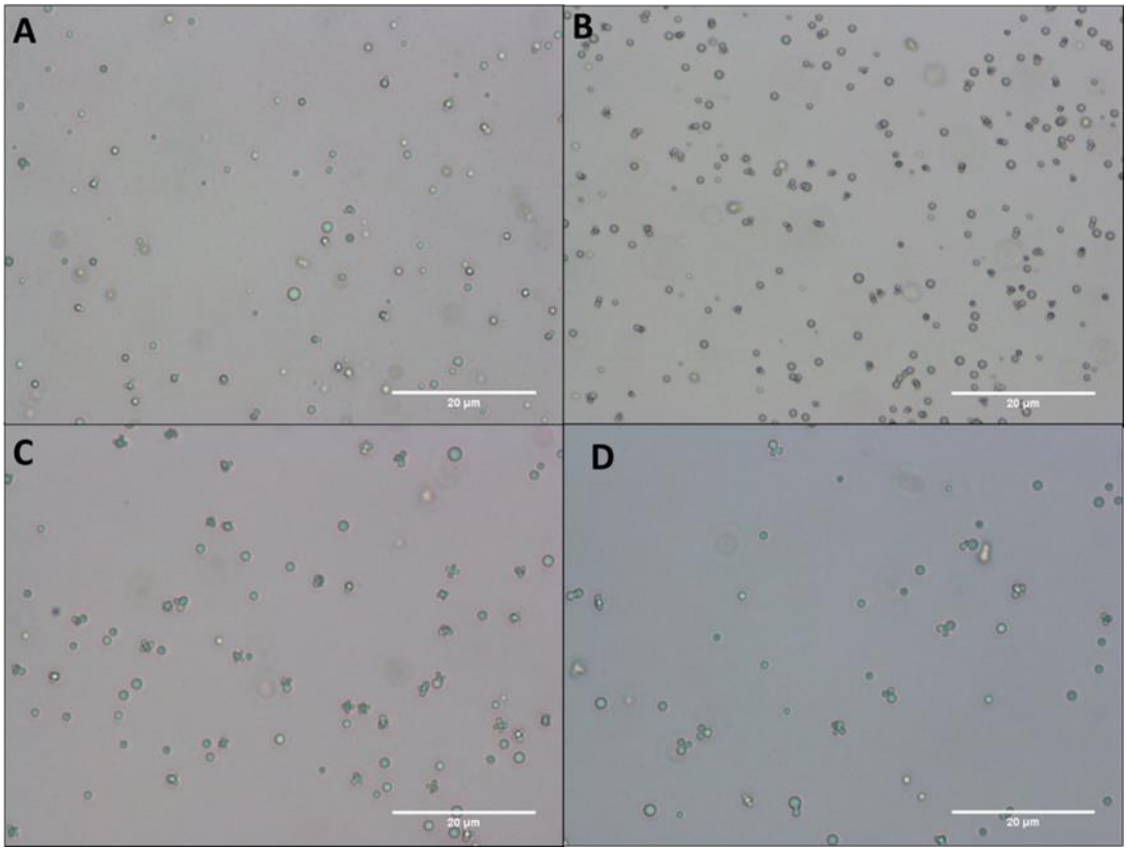

Figure 1.21*: Optical microscopy images showing the effects of temperature on the system with (a) showing sample I (b) sample II (c) sample III (d) sample IV.*

Table 3

Sample	TPM	MilliQ water	Polystyrene (0.3 wt.%)	Ammonia Solution (1 µL/mL)	Temperature
I	200 µL	1 mL	0.5 mL	10 µL	3°C
II	200 µL	1 mL	0.5 mL	10 µL	18°C
III	200 µL	1 mL	0.5 mL	10 µL	50°C
IV	200 µL	1 mL	0.5 mL	10 µL	85°C

1.4.3 Polymerisation Procedure

The first polymerisation procedure used involved solid radical initiator (AIBN) being added to the sample and then the sample being heated in an oven prior to polymerisation to allow the initiator to dissolve. This procedure yielded particles with fully rough surfaces, shown in Figure 1.22. The free TPM monomers left in the solution after the protrusion growth nucleate and crosslink over the entire particle. As the particles need to be fully smooth in order for their only capillary interactions to be a result of the particles shape anisotropy this polymerisation procedure is not suitable.

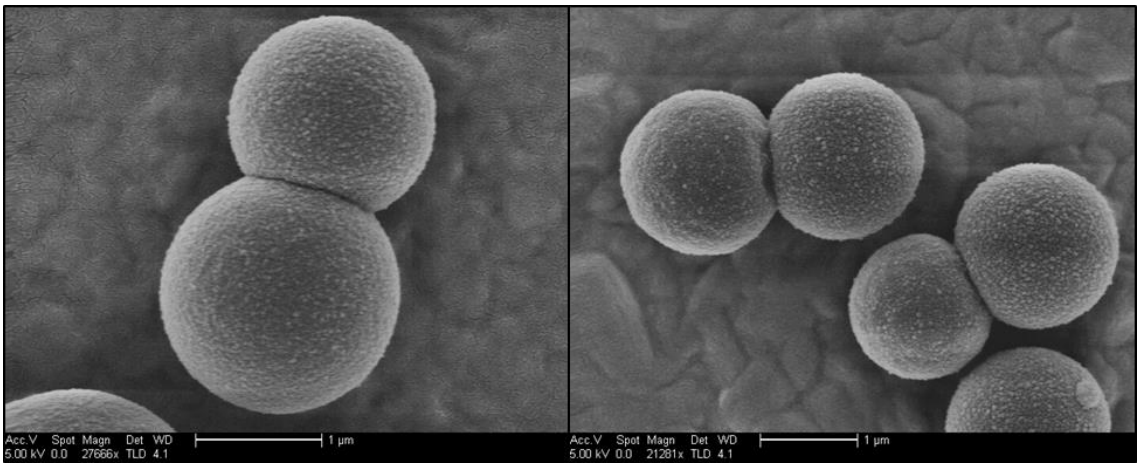

***Figure 1.22**: TEM images of anisotropic particles with rough surfaces from TPM formed during the polymerisation technique.*

For the next polymerisation procedure, a second batch of high concentration ammonia solution was added to the sample before polymerisation. It was hoped that this ammonia solution would use up all the free TPM monomers left in solution before polymerisation yielding a smooth particle. This procedure caused secondary nucleates of TPM on the polystyrene seed particle, shown in Figure 1.23. The TPM monomers preferentially nucleate on the polystyrene and form small protrusions. The small nucleates could be a result of the high concentration of ammonia used, meaning the nucleation procedure is a fast one, not allowing for time for nucleates to merge.

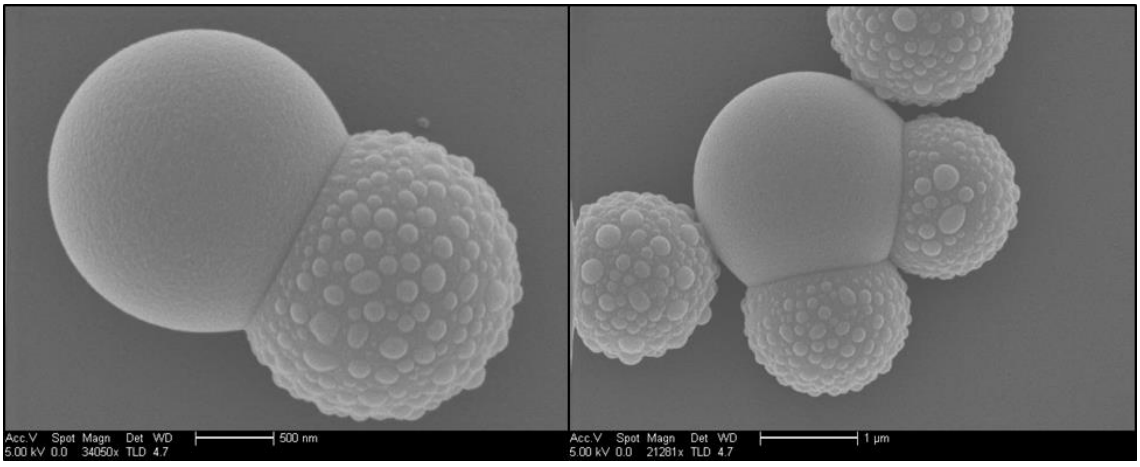

***Figure 1.23**: TEM image of dumbbell particle with fully smooth TPM lobe and rough polystyrene lobe with secondary nucleates.*

Another procedure used was to place the sample in the oven at 85 °C for 3 hours before adding AIBN salt. This yielded entirely rough particles, as shown in Figure 1.24, however they do seem to be less rough than the particles shown in Figure 1.22.

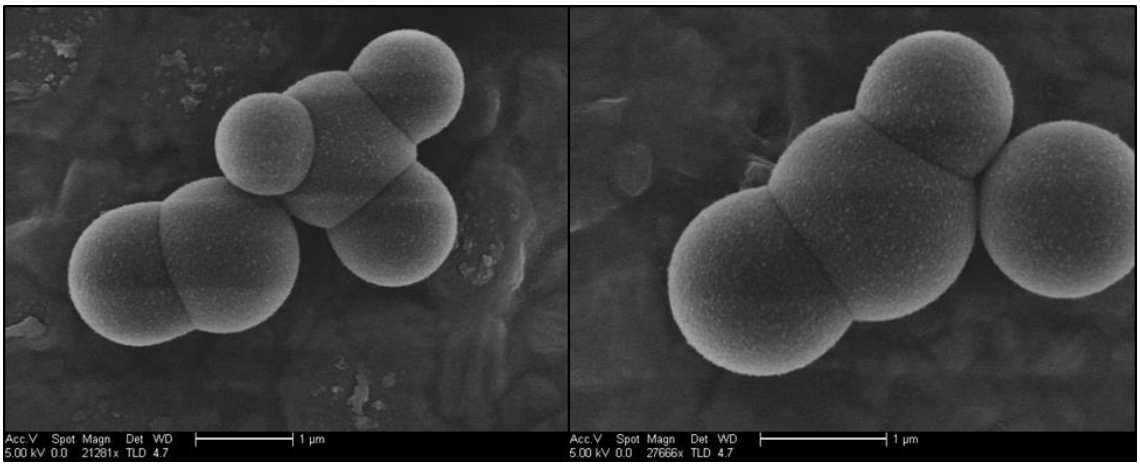

***Figure 1.24**: TEM images of anisotropic particles after polymerisation, covered in TPM monomers.*

The final polymerisation technique used was as follows: the solid AIBN was dissolved in a small amount of TPM oil and added to the sample. The resulting particles were much smoother than those from other polymerisation techniques, shown in Figure 1.25. As the initiator was dissolved in an oil, the initiator could have entered the TPM protrusion and the polymerisation procedure could have occurred from inside allowing the outside to stay smooth.

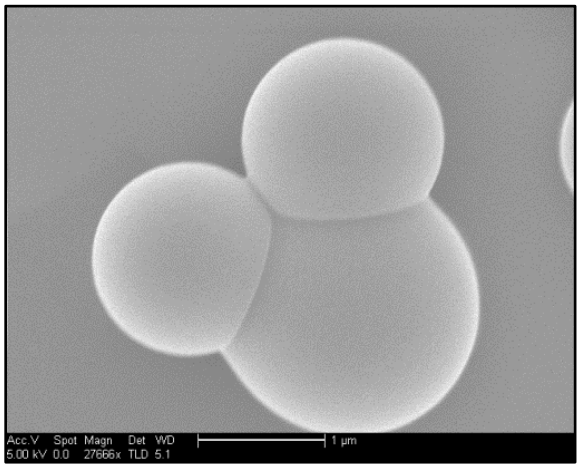

***Figure 1.25**: TEM image of Mickey Mouse shaped particle after polymerisation.*

1.4.4 Particle Separation

The density gradient centrifugation technique used was able to separate out some mixtures of particles into separate components. The sample shown below in Figure 1.26 consists of a mixture of many particle shapes including dumbbells and particles with 2 and 3 protrusions. The sample was placed upon a continuous gradient of 8-20 wt.% Ficoll and two bands were formed in the centrifuge tube after centrifugation.

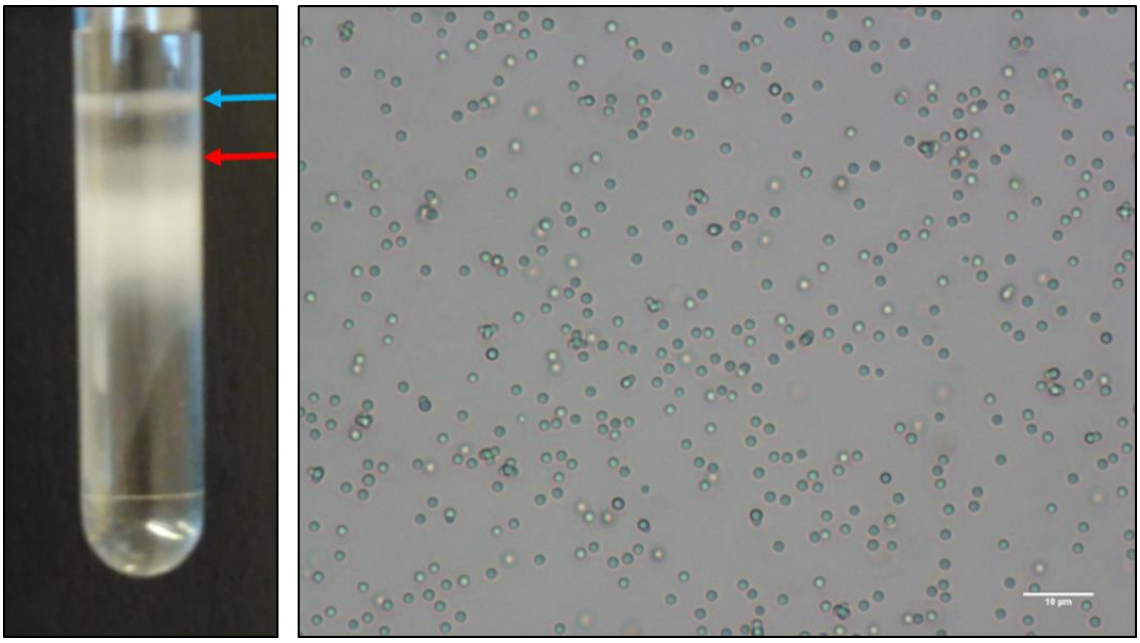

***Figure 1.26**: Density Gradient Centrifugation tube showing two bands of separated particles and optical microscopy image of the mixture of particles before separation.*

The top band, denoted by the blue arrow, contains only polystyrene particles with no protrusions and the lower band, shown with the red arrow, contains only dumbbell particles consisting of a polystyrene seed particle and a TPM protrusion, shown in Figure 1.27. The bulk of the samples could still not be separated using this technique and while a pure sample of dumbbell particles can be obtained the sample size is too small for this separation technique to be useful.

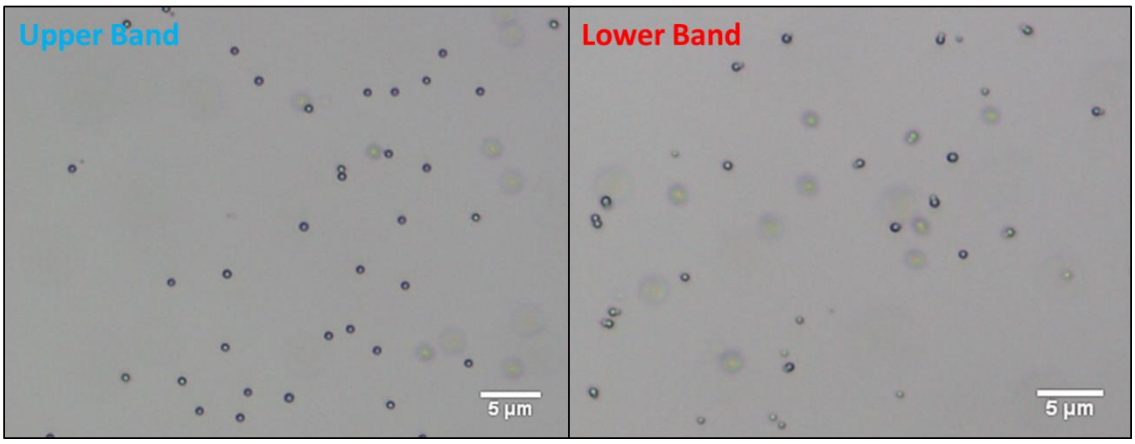

***Figure 1.27**: Optical microscopy image of the contents of the upper and lower bands shown in Figure 1.26 after separation. The upper band contains mostly polystyrene seed particles while the lower band is a pure solution of dumbbells.*

1.4.5 Hydrophobic Modification of TPM Protrusion

To test the hydrophobic modification procedure it was first carried out on TPM spheres. After the modification procedure the spheres are stable in bulk ethanol and do not form aggregates, seen in the optical microscopy image, Figure 1.28 A. Adding these TPM spheres to milliQ water resulted in large aggregates forming, showing the hydrophobicity of the particles surface, seen in Figure 1.28 B. When these particles were spread at a decane-water interface the expected stable lattice structure was not seen. Instead these particles strongly aggregated and formed disordered structures at the interface. This aggregation is shown in Figure 1.28 C.

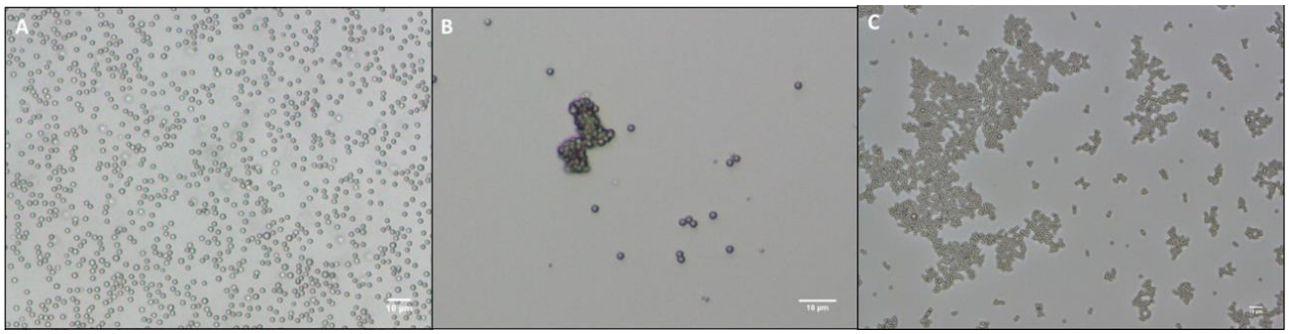

Figure 1.28: Optical microscopy images of hydrophobically modified particles (a) in ethanol (b) in water (c) at decane-water interface.

The driving force behind this aggregation at the oil-water interface is assumed to be lateral capillary interactions arising from surface roughness of the TPM spheres. This roughness is most likely induced during the polymerisation procedure of the TPM, as discussed above.

1.5 Conclusion and Outlook

This procedure to synthesis anisotropic particles is a complex one. Many parameters need to be controlled simultaneously and slight changes in conditions can affect the particle growth hugely. Polystyrene particles with single or multiple protrusions have been synthesised successfully and the structures formed can be controlled relatively well. By varying the concentration of TPM used the size of the protrusion can be tuned, with protrusion size increasing with increasing TPM concentration. Base concentration can also change the size of the protrusions formed, again with protrusion size increasing with base concentration. Temperature can affect the number of protrusions grown on the seed particle, with the number of protrusions increasing with temperature. This trend does not extend above 50 °C.

The challenges in this procedure lie in the separation and polymerisation steps. Every sample prepared had a mixture of particles with different numbers of protrusions, free TPM spheres and polystyrene particles. In order to use these anisotropic particles at the interface to form 2 dimensional structures by capillary interactions, a pure sample containing one type of particle is needed. This has been achieved with density gradient centrifugation and pure samples of dumbbells achieved. However, as this technique can only be carried out with a small amount of sample, it is not viable here.

The polymerisation step is the other hurdle for this procedure. All polymerisation techniques used produced particles with some type of roughness, either visible through TEM or on the nanoscale. This roughness on the TPM lobe induces capillary interactions, negating capillary interactions due to the shape of the particles.

Due to these two challenges, anisotropic particles that can form 2-dimensional structures at the interface could not be synthesised successfully.

In order to make this procedure a successful one a different polymerisation procedure needs to be employed. Preliminary results using an oil phase initiator have been successful. This initiator can enter in to the TPM lobe and allow for polymerisation from the inside, creating a smooth outer surface, see Figure 1.29. If smooth TPM protrusions can be formed, the particles could only be susceptible to capillary interactions induced by the shape anisotropy of the particle.

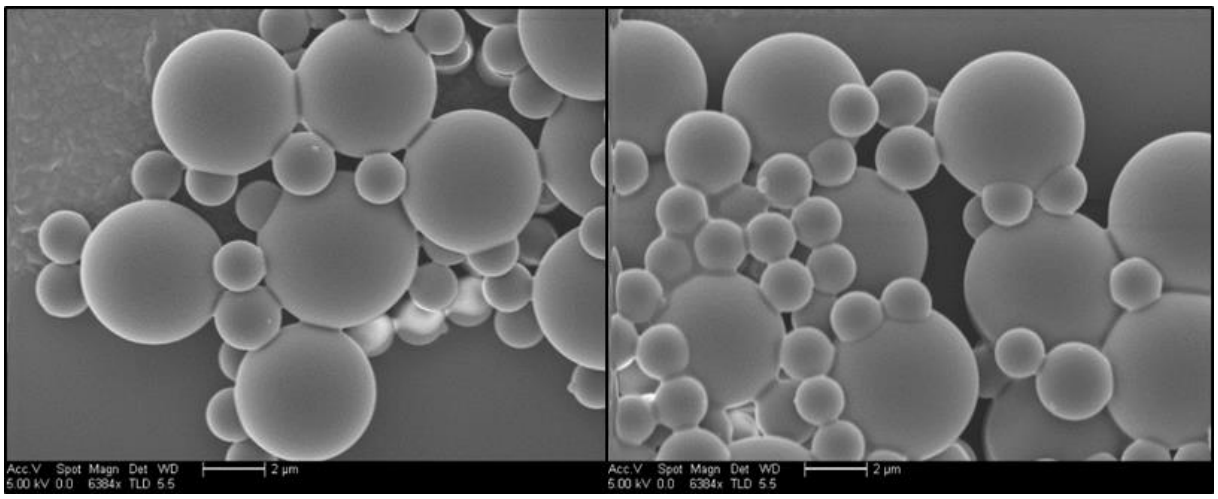

Figure 1.29: *TEM images of anisotropic particles using an oil phase initiator for polymerisation. The TPM lobes have much smoother surfaces than for the previous polymerisation techniques.*

2 Active Particles in 2-Dimensional Structures at the Oil-water Interface

2.1 Introduction

Active particles are ones which have the ability to take chemical energy from their environment and convert it into directed motion. The inspiration for these systems came from the countless examples of autonomous motion seen in nature, for example the self-propulsion of bacteria by flagella, which has been the subject of biomimicry in soft-matter systems. The field of active colloids has grown rapidly in recent times,[17] and considers colloidal particles which have the ability to move autonomously in a low Reynolds regime.

A particle in a fluid environment can move by Brownian motion but this movement lacks directionality. To induce a more directed motion an asymmetric conversion of energy around the particle to form local gradients is needed. These gradients create a route for the particle to travel along autonomously and can include changes in chemical concentration,[18] temperature[19] or light intensity.[20] In order for the symmetry breaking required to induce motion to be present, the active particle must possess some form of asymmetry. Janus particles can be employed for this reason. A Janus particle is one which has separate areas with different surface properties, either physical or chemical in nature. The nomenclature for these particles comes from the "two-faced" Roman god Janus.[21] The distinct surface properties can lead to particles that can possess more than one desirable property, for example amphiphilic particles can be created with a hydrophilic and a hydrophobic face.

In this research we utilise the most common and easily controlled method of inducing active motion of a particle, partial coating of the particle in platinum. The platinum coating acts as a catalyst in the decomposition of fuels, for example hydrogen peroxide. As an asymmetric distribution of products is formed around the particle, a local concentration gradient arises inducing motion of the particle.

Polystyrene spheres of approximately 5 μm in diameter partially coated in platinum are utilised as Janus particles here. The movement of these particles will be tracked in bulk, at an oil/water interface and confined in a 2-dimensional lattice structure at the oil/water interface, shown in Figure 2.1.

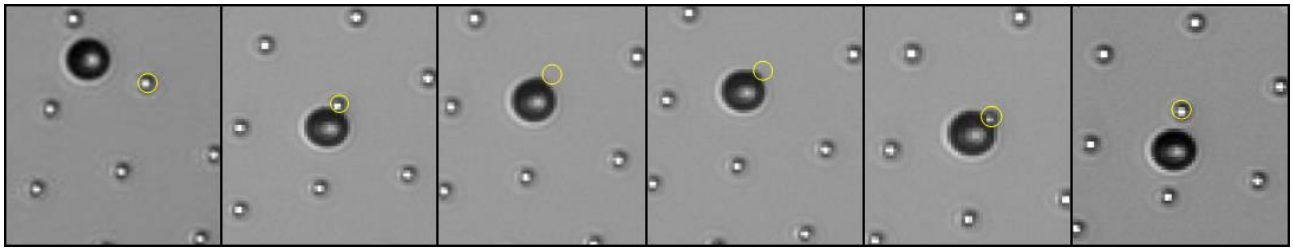

Figure 2.1: *Active particle (larger) moving through passive particles at oil-water interface.*

2.2 Theory

2.2.1 Active Particles

In order to see self-propulsion of microscale particles some boundaries must be overcome. The first boundary is the low Reynolds regime at which small particles at the microscale exist. Reynolds number (Re) is defined as the dimensionless ratio of inertial and viscous forces present in the system:

$$Re = \frac{\rho v L}{\mu} \qquad (2.1)$$

Where ρ is particle density, v is particle velocity, L is the characteristic length scale of an object and μ is the viscosity of the surrounding medium. For microscale particles the inertial forces decrease, due to a decreasing L, and become negligible as viscous forces dominate. In order for the particles to overcome the viscosity of the solution and self-propel, a constant force must be applied to the particle.[22] This force can come in the form of symmetry breaking and the creation of local gradients.

The most reproducible and easy to control method of inducing movement of a particle is the platinum catalysed decomposition of hydrogen peroxide to form dioxygen and water ($2H_2O_{2(l)} \rightarrow O_{2(g)} + 2H_2O_{(l)}$).[18] Howse *et al.* [23] showed that for polystyrene particles with an asymmetric coating of platinum catalyst in a dilute hydrogen peroxide solution, as depicted in Figure 2.2, the particle will take directed motion at short time scales before reverting to a random-walk. This reaction creates local chemical concentration gradients inducing self-propulsion of the particle. This movement by a chemical gradient is referred to as *self-diffusiophoresis*.

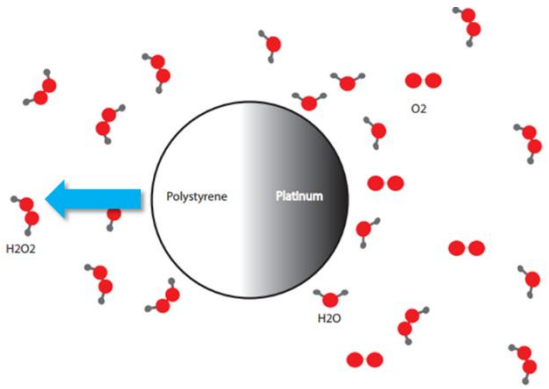

***Figure 2.2**: Decomposition of hydrogen peroxide to water and dioxygen with a platinum catalyst on a polystyrene sphere. The blue arrow shows the expected direction of movement of the Janus particle.*

Ke *et al.*[24] studied the motion of 1 μm platinum coated silica spheres and, by using optical microscopy, concluded that the motion of the particles in the opposite direction to the Pt side, as per Figure 2.2. As more products are formed at the platinum coated surface, a higher chemical concentration is formed here which is thought to push the particle away in the opposite direction.

The authors also observed a ballistic regime at short time scales and an enhanced Brownian motion at times longer than the rotational diffusion time. This self-diffusiophoresis is only valid for particles of less than 5 μm.

For particles larger than 10 μm, bubble propulsion is thought to be the method of motion. The proposed mechanism is as follows: microbubbles of oxygen form at the platinum coated surface, the microbubbles grow in size until they are released and induce motion of the particle by their detachment.[18] This is still under investigation and it is unclear if this proposed mechanism is the correct one.

The active particles utilised in this report are polystyrene particles with a radius of approximately 5 μm, semi-coated in platinum, so can be assumed to undergo self-diffusiophoresis.

2.2.2 Mean Squared Displacement

To characterise the motion of the active particles we calculate the mean squared displacement (MSD) of the particle. The MSD is a mean measure of how far a particle travels in a given time step in reference to a fixed point and can generally be defined as:

$$MSD = \langle (r - r_0)^2 \rangle = \frac{1}{N} \sum_{n=1}^{N} (r_n(t) - r_n(0))^2 \qquad (2.2)$$

where N is the number of particles to be averaged, $r_n(t)$ the position of the particle at time t and $r_n(0)$ the reference position of each particle.

Along with directed active motion the particle simultaneously undergoes Brownian motion, due to thermal fluctuations, which can be characterised by its diffusion coefficient D_0, from the Stokes-Einstein relation:

$$D_0 = \frac{k_B T}{6\pi\eta R} \qquad (2.3)$$

Where R is the radius of a spherical particle, η is the viscosity of the surrounding medium, k_B is the Boltzmann constant and T the temperature in kelvin.

Howse *et al.*[23] described the full range of motion taken by an active particle in 2-dimensions by combining the active and Brownian motion:

$$MSD = \langle r^2 \rangle = 4D_0 \Delta t + \frac{V^2 {\tau_r}^2}{2} \left[\frac{2\Delta t}{\tau_r} + e^{-\frac{2\Delta t}{\tau_r}} - 1 \right] \qquad (2.4)$$

Where D_0 is particle diffusion coefficient, τ_r is rotational time, V is particle velocity.

At short time scales, with $t \ll \tau_r$, the equation has the limiting form:

$$\langle r^2 \rangle \approx 4D\Delta t + V^2 \Delta t^2 \qquad (2.5)$$

Here MSD scales with t^2, indicating a non-diffusive, directed movement of the particle, this regime is described as super-diffusive and will show an increasing slope.

At longer time scales, $t \gg \tau_r$, the equation becomes:

$$\langle r^2 \rangle \approx (4D + V^2\tau_r)\Delta t \qquad (2.6)$$

Showing the particle moving into a diffusive regime as MSD scales with time, this plot shows a linear slope as seen for a particle only undergoing Brownian motion.

2.2.3 Active Particles at Interface

While little work has been done on active colloids at oil-water interfaces, swimmers at air-water interfaces have been studied. Wang *et al.* [25] showed that by trapping an active particle at the air-water interface its directional motion can be greatly enhanced. The pinning of the colloidal particle at the interface slows down the rotational motion, forcing the particle to take longer linear trajectories and preventing the frequent changes in direction possible in bulk, see Figure 2.3. The reduction in rotational freedom is attributed an interfacial friction which adds to the overall hydrodynamic friction on the particle. This two dimensional confinement of the swimming particles also increases the particles velocity of propulsion.

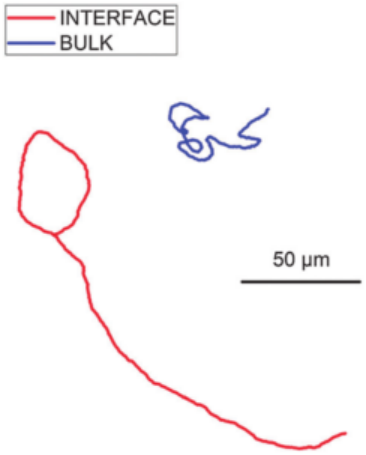

Figure 2.3: *The trajectories an active particle takes in bulk and confined at an air-water interface. The more linear motion at the interface is attributed to the slowing down of rotational motion. From Figure 2 in [25].*

The orientation of the particle at the interface is an important factor to consider when analysing the motion of these active particles. In order for swimming to be seen, a section of the platinum coating on the particle must be immersed in the aqueous phase (hydrogen peroxide solution). It is likely for the platinum coating to pin strongly to the interface due to its inherent roughness. Park *et al.* [26] have studied the orientation of Janus particles at oil-water interfaces by utilising polystyrene particles semi-coated with gold (PS-Au). The gold surface was modified, using dodecanethiol and octadecanethiol, to increase hydrophobicity in order to investigate the effect of wettability on the particles orientation. Their results, shown in Figure 2.4, show that for PS-Au

particles which have not been modified the majority of the particles (~55%) have the entire gold hemisphere immersed in the oil phase. The remaining particles have some section of the gold coating in the aqueous phase, either a fraction of the coating (~30%) or the entire gold hemisphere (~15%). As the hydrophobicity of the gold layer is increased, a high majority of the particles have the entire gold hemisphere sitting in the oil phase (>90%).

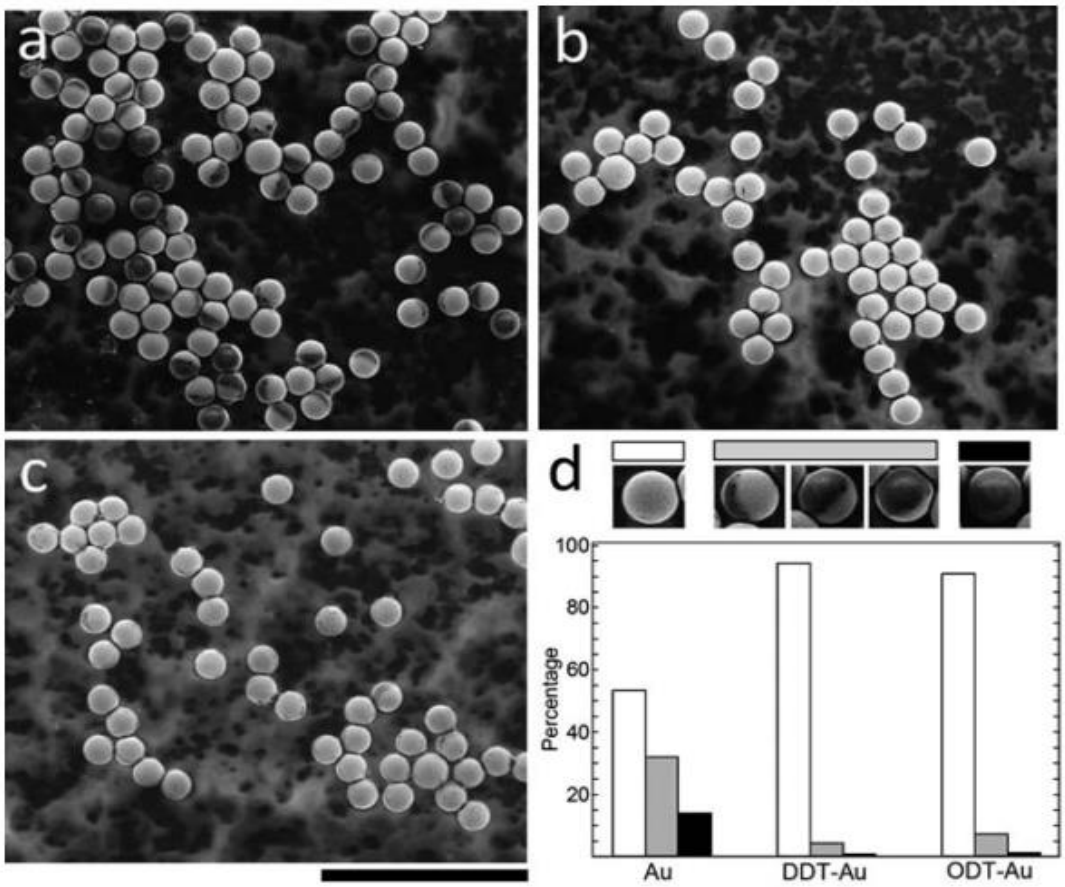

Figure 2.4: *SEM images showing (a) PS-Au (b) PS-Au with gold coating modified with 1-dodecanethiol (c) PS-Au modified with 1-octadecanethiol and the orientation these particles take at the oil-water interface. (d) Histogram of particles orientation at interface, determined from SEM images, with the white bar corresponding to particles the gold region fully in the oil phase, the gray bar representing particles with a tilted conformation and the black bar showing particles with the gold region in the aqueous phase. From Fig. 2 in [26].*

In addition to the wettability of the particle, the roughness of the particle can also affect the orientation at the interface. The boundary between the two sections of the Janus particle will be rough when a sputter coating technique, such as used in this report, is employed. The roughness can induce pinning at this boundary with the particle in either orientation, shown in Figure 2.5 A,B. The sputter coating technique also causes the metal-coated side of the Janus particle to have an inherent roughness, which could lead to pinning of the particle just below the interface, shown in Figure 2.5 C,D.

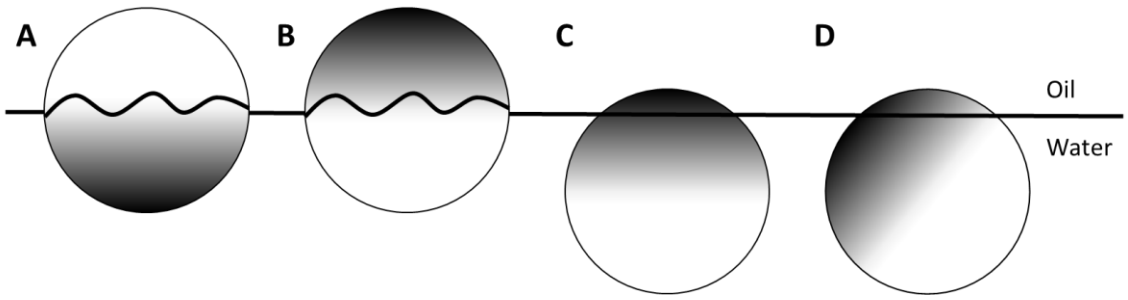

Figure 2.5*: Different orientations Janus particles could take at the interface due to roughness effects. (a), (b) roughness of the Janus boundary could lead to particles being preferentially pinned with each hemisphere immersed in a different phase. (c), (d) inherent roughness created through the sputter coating technique could lead to the metal coated side being pinned just under the interface.*

In order to determine the orientation of Janus particles at the interface, a gel trapping technique is utilised. This technique is adapted from the method of Paunov,[27] and uses the procedure outlined in Figure 2.6. We replace the aqueous phase with Gellan, a hydrocolloid polymer which forms a gel at room temperature and has no surface activity at the oil-water interface. The oil phase is then replaced with a poly(dimethylsiloxane) silicone elastomer (PDMS), which is cured and removed from the water phase. The interfacial particles are then sitting on the PDMS layer with their interfacial orientations preserved, which can be imaged by SEM to determine the orientation.

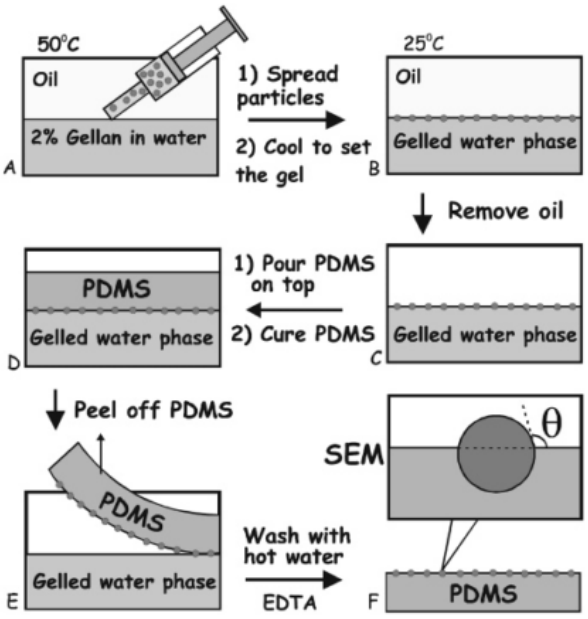

Figure 2.6*: Gel trapping technique used to measure the orientations of the Janus particles at the interface. From Figure 1 in [27].*

2.2.4 Repulsive Interfacial Interactions

As mentioned in chapter one, particles at the interface have attractive and repulsive forces acting on them. In chapter one the attractive forces of van der Waals forces and capillary interactions were introduced, here the repulsive forces which stabilise the particles at the interface are discussed.

Monolayers at Interface

Charged particles adsorbed at oil-water interfaces have been shown to form stable lattice structures with a high degree of uniformity.[11][28] The presence of these stable lattices shows a long range repulsive interaction must be at work over the interface. According to Pieranski, the repulsive forces present here are dipolar interactions through the water phase.[29] As only a section of the polystyrene particle is immersed in the polar phase, the surface charges are distributed asymmetrically around the particle due to dissociation of the sulfonic acid groups. Thus leading to a dipolar moment forming perpendicular to the interface, shown in Figure 2.7.

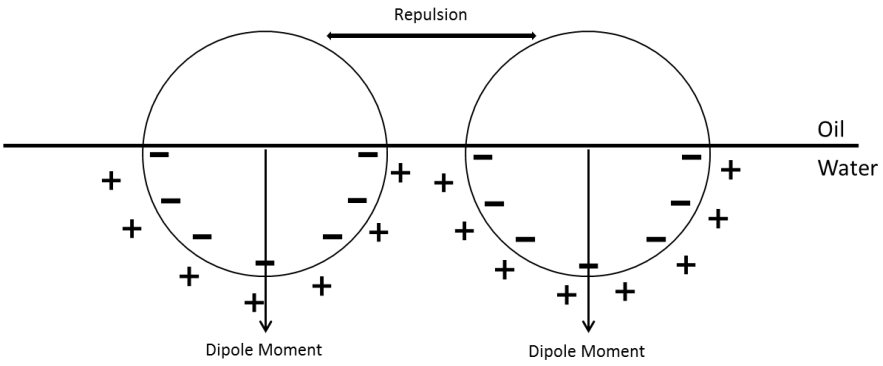

***Figure 2.7**: The asymmetric charge distribution around particle at the interface due to the dissociation of sulfonic acid groups on the polystyrene surface immersed in the water phase.*

Some charges could also be present on the particles surface in the oil phase which could lead to long-range Coulomb repulsions arising from charges present at the particle-oil interface from polar surface groups.[30] These charges can arise from the spreading agent that's employed to transport the particles to the interface. For example, if ethanol is used and some remains on the surface of the particle as it sits at the interface, polar hydroxyl groups can induce these long-range coulombic interactions. However, the majority of the repulsion has been shown to take place through the water phase,[31] with a full understanding of the oil phase interactions still unknown.

2.3 Materials and Methods

2.3.1 Materials

Chemical	Source
2,2′-Azobis(2-methylpropionitrile)	Fisher Scientific

Chemical	Source
Hydrogen peroxide (35 wt.%)	Fisher Scientific
4-Styrenesulfonic acid sodium salt hydrate (Mw=206.19)	Aldrich
Divinylbenzene (80%)	Aldrich
Styrene (≥99%)	Sigma-Aldrich
Decane (≥99%)	Sigma-Aldrich
Ethanol (ACS ISO reagent)	Emsure
Methanol (≥99%)	Biosolve
Gellan gum	VWR International
Polydimethylsiloxane (Mw=47,500)	Mavom

All water used has been filtered through a MilliQ® water purification system. 5 µm polystyrene particles were obtained from Daniël ten Napel. Decane was purified by removing the polar components by adsorption onto aluminium oxide powder.[16] All other chemicals were used without further purification.

2.3.2 Polystyrene Particle Synthesis

Polystyrene particles were used to create a stable lattice structure at the oil-water interface. The polystyrene particles used are the same particles utilised in Chapter 1 and are synthesised via the same method as described in section Synthesis of Polystyrene Seed Particles.

2.3.3 Preparation of Janus Particles

The following procedure was used to prepare Janus particles of 5 µm polystyrene particles semi-coated with platinum. Firstly, a 2 wt.% solution of 5 µm polystyrene particles in ethanol was prepared. A 100 mL beaker was partially filled with milliQ water and a glass slide placed below the surface of the water using the experimental set up shown in Figure 2.8. 30 µL of polystyrene solution was then added slowly to the surface of the water, allowing for the formation of a monolayer of particles on the water surface. The water was pumped out of the beaker from its base at a rate of 48 rpm, using a Gilson Minipuls 3 pump, until the surface of the water was below the glass slide. The glass slide, now containing a monolayer of particles, was removed from the beaker and its underside cleaned with ethanol to remove excess particles.

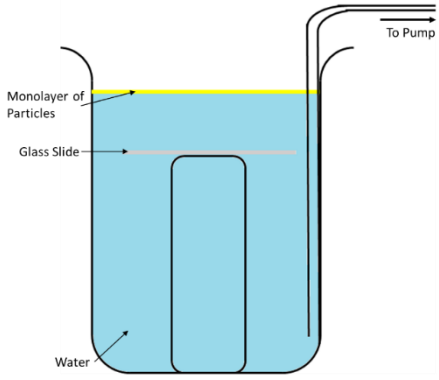

Figure 2.8: *Monolayer formation experimental set up.*

A sputter coater with a platinum target was used to coat the particle monolayers. The glass slides were placed on the stage of a Cressington 108 sputter coater and the reaction chamber flushed with argon gas and evacuated to 0.08 mbar. The coating procedure was then allowed to occur for 200 seconds to create a 10 nm thick layer of platinum on the exposed section of the monolayer. To redisperse the Janus particles, the glass slides were then placed in a beaker with 3 mL of ethanol and sonicated for 3 minutes to remove the particles from the substrate. The ethanol containing the particles was transferred to an Eppendorf tube and centrifuged at 11,000 rpm for 3 minutes. The supernatant was removed and replaced with fresh ethanol, and the centrifugation repeated. This washing procedure was carried out three times before redispersal of the Janus particles in ethanol.

2.3.4 Interfacial Experiments

The fluid cell described in 1.3.7 is also utilised for these experiments.

To observe the Janus particles at the interface, 2 μL of a suspension of Janus particles in ethanol was injected just below the interface and the particles allowed to spread at the interface. To observe the Janus particles in a lattice structure at the interface, 5 μL of a 0.2 wt.% solution of 1 μm polystyrene particles in ethanol was injected below the interface. Following this 2 μL of a suspension of Janus particles in ethanol was injected just below the interface. For the active particle experiments the aqueous phase consisted of a 5 wt.% hydrogen peroxide solution. This solution was prepared by diluting 1.4 mL 35 wt.% hydrogen peroxide with 8.6 mL milliQ water.

A motorised Nikon Ti Eclipse inverted optical microscope was used to image the interface, with a Nikon 60x air objective with a working distance of 1.3 mm. The microscope is controlled by NIS Elements software and videos of an .nd2 format were recorded.

2.3.5 Particle Position at Interface Determination

In order to observe the position of the particles at the oil-water interface the following procedure was used, adapted from [27]: a 2 wt.% Gellan solution was prepared by dissolving 100 mg of Gellan in 5 g milliQ water. This solution was heated to 95 °C in an oil bath for 15 minutes to allow the gel to liquefy, along with a vial containing 1 mL decane. The fluid cell was placed in an 85 °C oven for 20 minutes to prevent Gellan from solidifying immediately upon contact with the glass. The oil-water interface was then prepared as described above using 2 wt.% Gellan as the aqueous phase. 5 μL Janus particles in ethanol solution was injected slightly below the interface. The cell was then left at room temperature for 30 minutes to allow the gel phase to fully set. A polydimethylsiloxane (PDMS) solution was prepared by adding 1g of curing agent to a 100 mL centrifuge tube containing 10 g polydimethylsiloxane and mixing thoroughly. The PDMS solution was centrifuged for 15 minutes at 7400 rpm to allow dust to settle at the base of the tube. The decane was then removed from the fluid cell with a syringe and any reside soaked up with the edge of a tissue paper. 0.8 mL PDMS solution was then added on top of the Gellan in the fluid cell using a positive displacement pipette, shown in Figure 2.9. The PDMS was left to cure for 48 hours and then peeled off the Gellan layer. The PDMS layer was washed in 95 °C milliQ water for 10 minutes to remove any Gellan residues. The sample was then imaged using SEM.

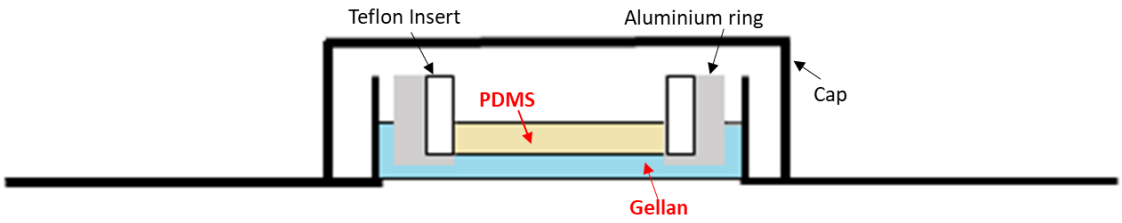

***Figure 2.9**: Fluid cell with Gellan replacing the aqueous phase and PDMS replacing the oil phase.*

2.3.6 Analysis of Particle Tracking

Analysis of the particles movement was tracked using MATLAB (version R2016b). The .nd2 videos were converted to 8-bit TIFF stacks using ImageJ software before being loaded into MATLAB. The particle tracking code is shown in Appendix 1.

2.4 Results and Discussion

2.4.1 Janus Particle Synthesis

Uniform Janus particles consisting of 5 µm polystyrene particles with one hemisphere coated in platinum were produced. Optical microscopy was used to confirm the coating procedure was successful. In Figure 2.10, the platinum coated section of the particle is evident as the darker side of the particle, as less light can penetrate this section of the particle.

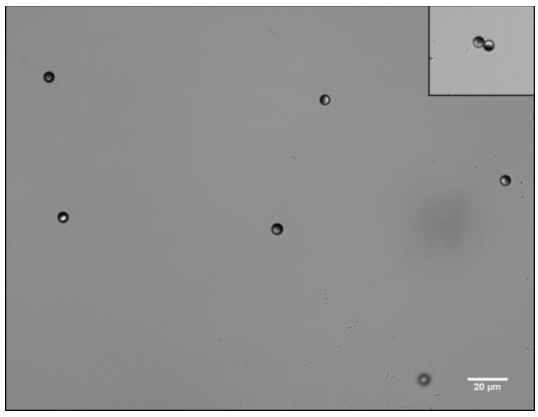

***Figure 2.10**: Optical Microscopy image of Janus particles in water, with platinum coating on the darker side of the particle.*

The Janus particles movement in a solution of 5 wt.% hydrogen peroxide solution was then measured. The particles imaged were sitting just above the glass base of the cell and their self-propulsion was evident. In Figure 2.11 A, an averaged mean squared displacement (MSD) plot of the particles movement shows an increasing slope which scales with t^2 which is characteristic of an active particle. The slope scales with a cubic function and does not reach long enough time scales to see a switch in behaviour from directed to diffusive. The log plot of the MSD, in Figure 2.11 B, has an initial slope of approximately 2.5 which decreases to approximately 1.67 at longer

time scales. The track diagram, in Figure 2.12 B, shows the tracks active particles took over a video of 30 seconds, showing the particles are not just undergoing Brownian motion but also a directed motion. The plots do not show linear movement with the particle able to rotate and change direction freely in the bulk solution. The circling of the particles could be due to imperfections in the platinum coating.

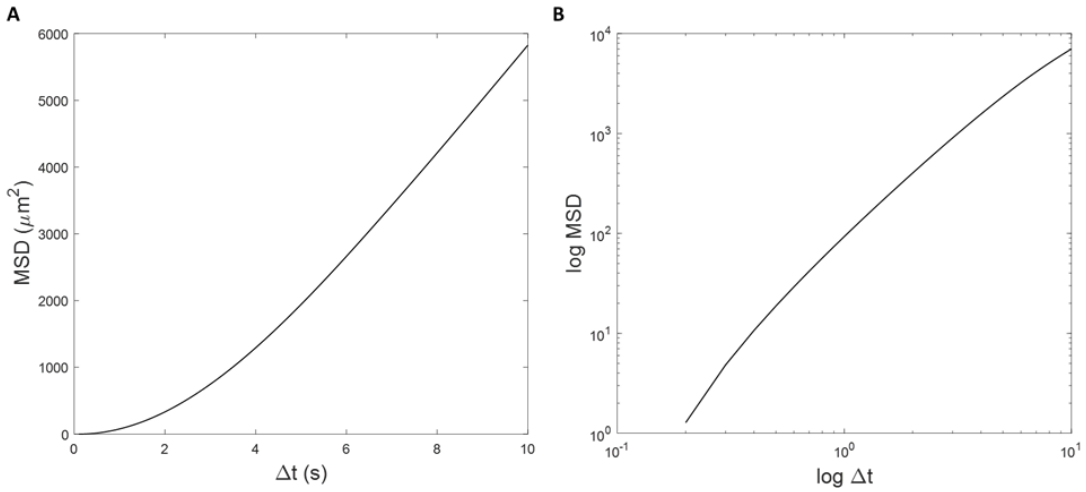

Figure 2.11*: A: MSD plot for Janus particles in bulk hydrogen peroxide, scales with a cubic function. B: Log plot of MSD of active particles with an initial slope of 2.51 which decreases to 1.67 at longer time scales.*

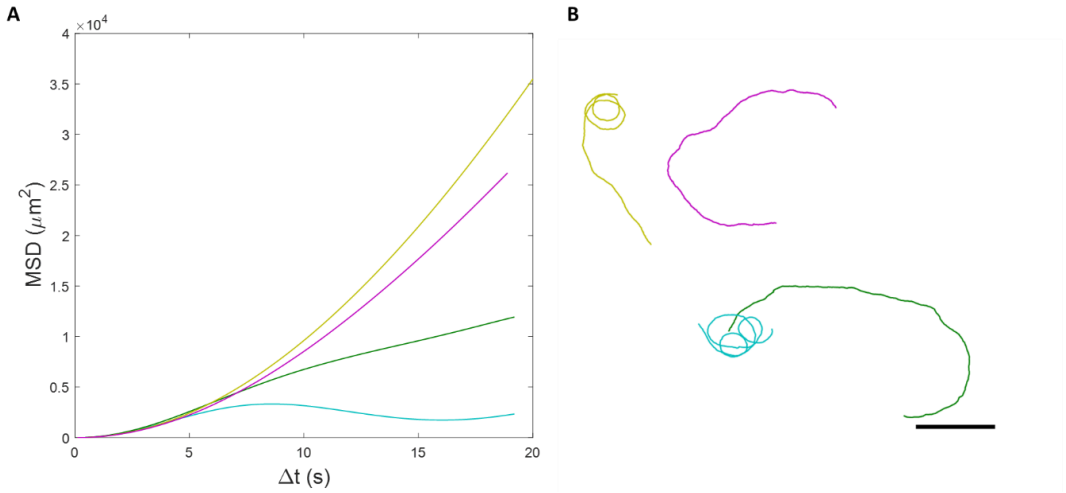

Figure 2.12: *A: MSD of four single particles, the plots agree well initially before diverging at longer time scales. B: Trajectories of active particles which seem to take a circular motion.*

2.4.2 Janus Particle at Oil-Water Interface

The movement of the active particles at a decane-hydrogen peroxide interface was then tracked. All the following experiments were performed with a 5 wt.% hydrogen peroxide solution. Figure 2.13 A shows MSD plot of the active particles, with an increasing slope evidencing their ability to

still self-propel at the interface. Figure 2.13 B shows a log plot of the MSD with an initial slope of 2.01 before transitioning to a slope of 1.73 at longer time scales.

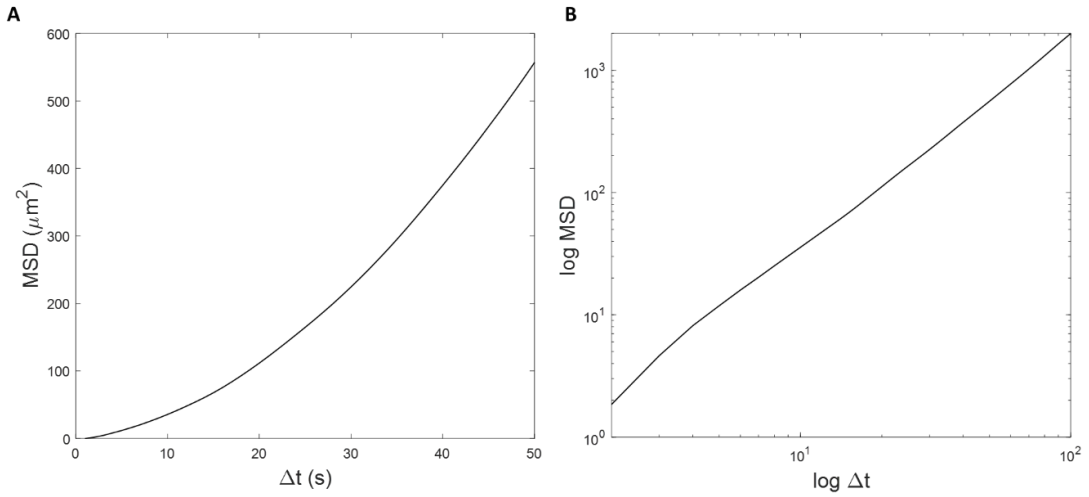

***Figure 2.13**: A: Average MSD plot of active particles at interface. B: Log plot of MSD of active particles at the interface with an initial slope of 2.01 and a slope of 1.73 at longer time scales.*

A plot of the tracks the particles took is shown in Figure 2.14. These tracks are not as linear as expected from results in [25]. This could show that the particles are trapped slightly below the interface so retain some of their rotational motion. The results from [25] are taken at an air-water interface rather than the oil-water interface utilised in these experiments. The separate MSD plots are shown in Figure 2.14. There is a big difference between these plots so the error is shown in Appendix 5.2.

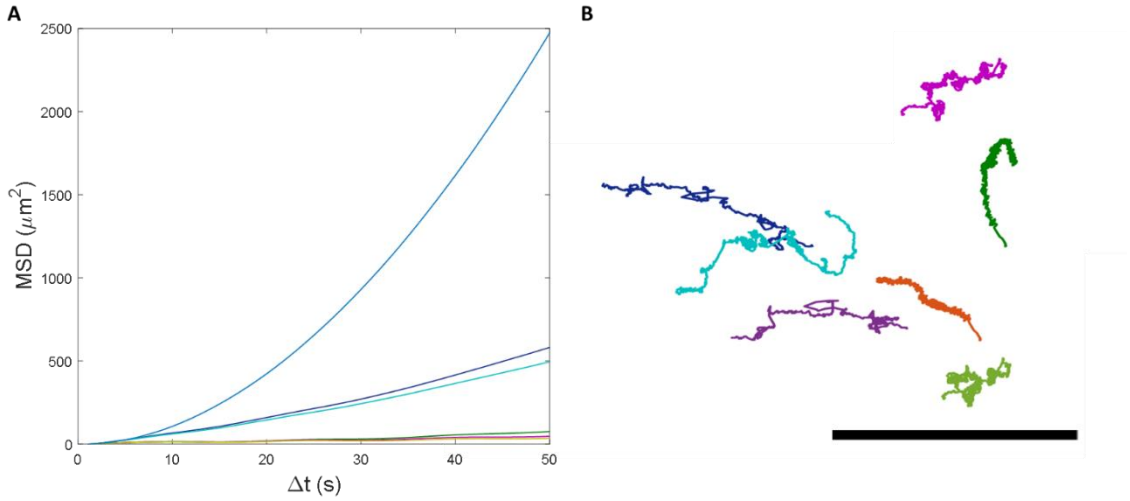

***Figure 2.14**: A: MSD plots of 7 single active particles at oil water interface B: Tracks of active particles at glass base of cell.*

2.4.3 Lattice Structures at Interface

Upon addition of 1.5 μm uncoated polystyrene particles to the interface, a 2-dimensional lattice structure was formed, shown in the optical microscopy image in Figure 2.15. The lattice was well ordered and stable with some dimers present, and displayed a hexagonal conformation with a separation of approximately four particle diameters. This structure forms due to the long range repulsive interactions at the interface.

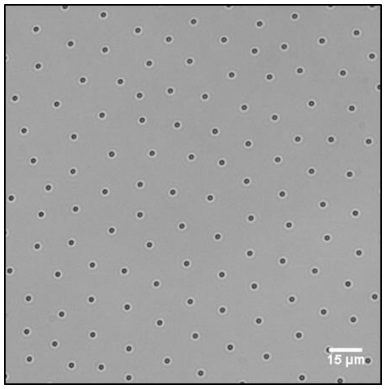

***Figure 2.15**: Optical microscopy image of polystyrene lattice structure at oil-water interface.*

2.4.4 Janus Particles in Lattice Structures at Interface

Active particles were then added to the lattice structure at the interface to measure how the lattice affected the motion of the particle and if the lattice's structure could be affected by the movement.

If the water phase does not contain any fuel, i.e. a 0 wt.% H_2O_2 solution, the active particles will not swim. This is shown by the linear MSD plot of an active particle in the lattice with no fuel present, in Figure 2.16 A, which confirms only diffusive motion of the particles is occurring. Figure 2.16 B shows a log plot of the MSD, which has a slope of 1 showing only Brownian motion is present here. This shows the lattice is not inducing any movement of the active particle.

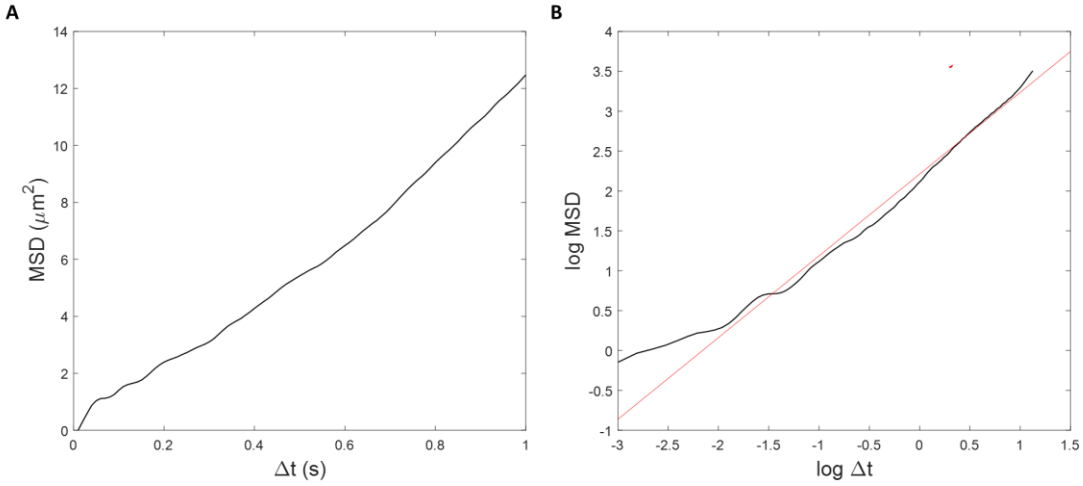

***Figure 2.16**: A: MSD plot swimming particle in lattice with no fuel in water phase B: log plot swimming particle in lattice with no fuel in water phase, the trend line of the data has a slope of 1.*

If the aqueous phase is 5 wt.% hydrogen peroxide, the Janus particles self-propel through the lattice structure at the interface. Their trajectories, shown in the plot of the tracks in Figure 2.18 B, are much more linear than the plots for the active particles at the interface with no lattice, in Figure 2.14 B. The active particles travel along straight lines of the lattice particles or along tracks between two parallel lines of particles. The log plot of the MSD of the active particles is shown in Figure 2.17 has a slope of 2.07.

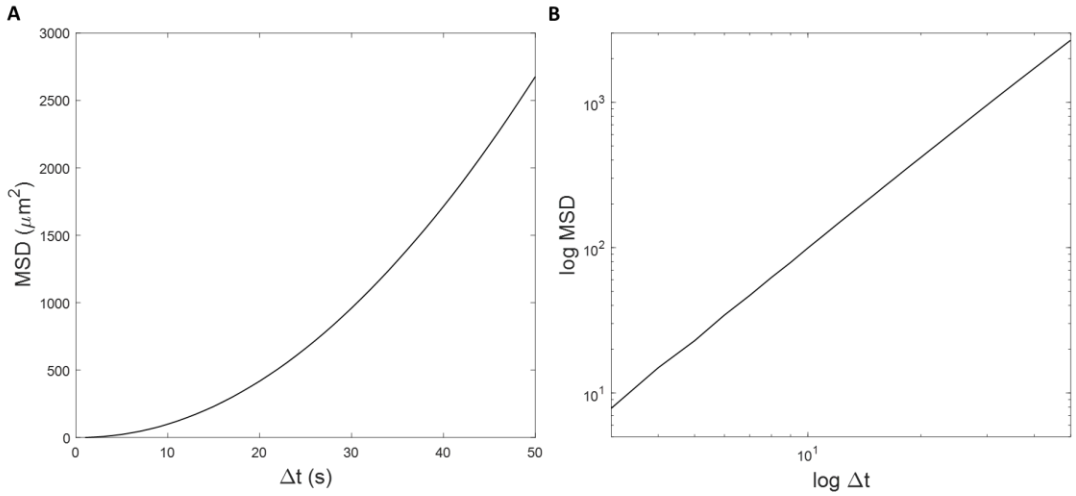

***Figure 2.17**: A: Average MSD active particles with lattice at interface showing directed motion. B: Log plot of MSD of active particles with lattice, with a slope of 2.07.*

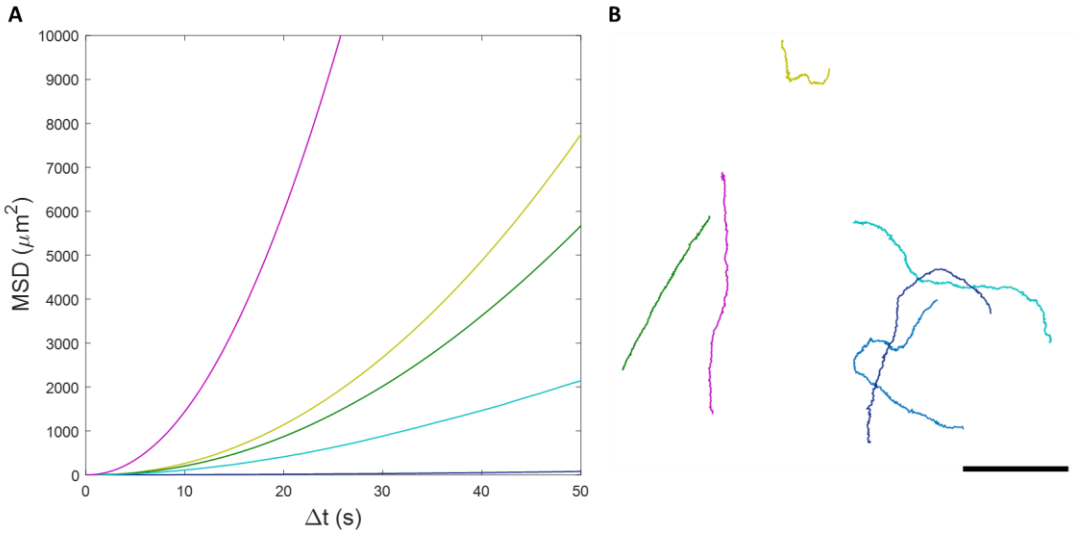

***Figure 2.18**: A: MSD of five single active particles with lattice at interface. B: Tracks of active particles at interface with lattice structure present.*

A comparison of the MSD plots of the active particles at the interface with and without the lattice particles is shown in Figure 2.19 A. From this plot it is evident the MSD of the active particles is increased by the lattice particles at the interface. At t=50, the MSD of the particles with a lattice present is approximately 2600 μm^2 while for the particles with no lattice the MSD is approximately equal to 550 μm^2. The slope of the log plot also increases by addition of the lattice structure to the interface, from m=1.73 for swimming with no lattice to m=2.07 for swimming within a lattice. This shows the increase in velocity for lattice swimmers, which could be due to the lattice structure steering the particles on more linear tracks preventing directional changes which slow down the particle, unlike the more random movement the particle takes when no lattice structure is present. The initial slope of the particles swimming with no lattice present is 2.01, showing that the velocity of the particles on a short time scale does not change due to the presence of a lattice structure.

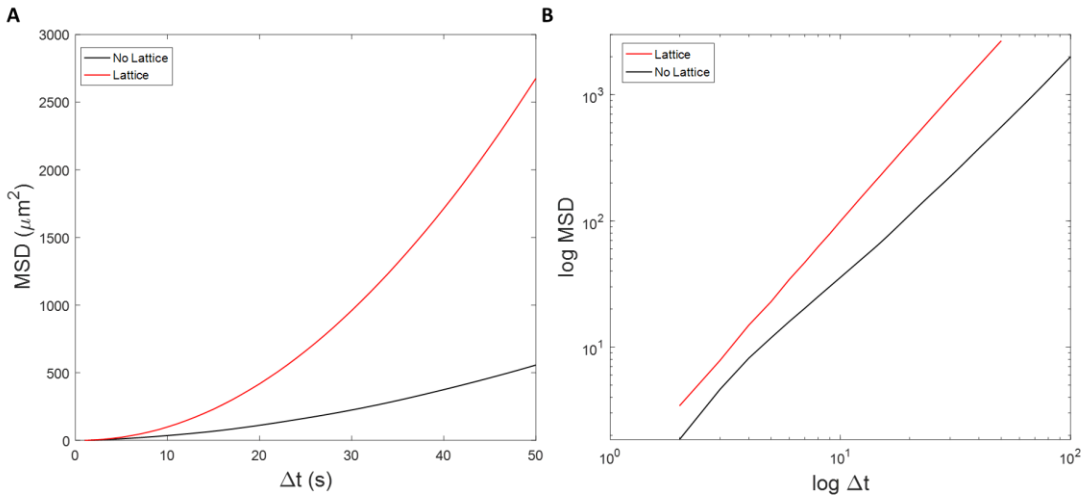

Figure 2.19: *A: Average MSD of active particles with lattice present (red) and without lattice (black). B: log plots of MSD for lattice (m=2.07) and non-lattice (initial m=2.01, m=1.73) particle.*

The trajectories of the swimming particles at the interface were also analysed by calculating the distance travelled and the number of direction changes per unit time, shown in Table 4. The swimmers with no lattice particles present travel a shorter distance than the swimmer which move through the 2 dimensional lattice. The velocity of the swimmers with no lattice is, on average, half that of the lattice swimmers. The number of direction changes per second is almost equal for the two different swimming regimes. But, as the particles velocity is higher in the lattice, the lattice swimmers travel a further distance before changing direction than the non-lattice particles.

Table 4

	Direction Changes (s^{-1})	Velocity (μm/s)	Distance Travelled Before Direction Change (μm)
Swimmers with No Lattice	0.051	5.077	79.299

	Direction Changes (s^{-1})	Velocity (μm/s)	Distance Travelled Before Direction Change (μm)
Swimmers with Lattice	0.049	11.725	92.030

This shows that the interfacial lattice structure has an unexpected effect on the swimmers movement. Although the particles are meeting obstacles, their velocity is increasing instead of decreasing. This could be due to the lattice particles steering the particles trajectories into a more linear movement. The lattice swimmers travel longer distances linearly before changing direction allowing for a higher velocity before the direction change slows the velocity.

2.4.5 Movement of Swimmer in Lattice

The active particles moving through the lattice show a catch and release mechanism with the lattice particles, illustrated in Figure 2.20. As the active particle moves toward the lattice particle the lattice particle is pulled momentarily from its position before being released again and returning to its original position. The lattice particles move approximately one particle diameter from its lattice position.

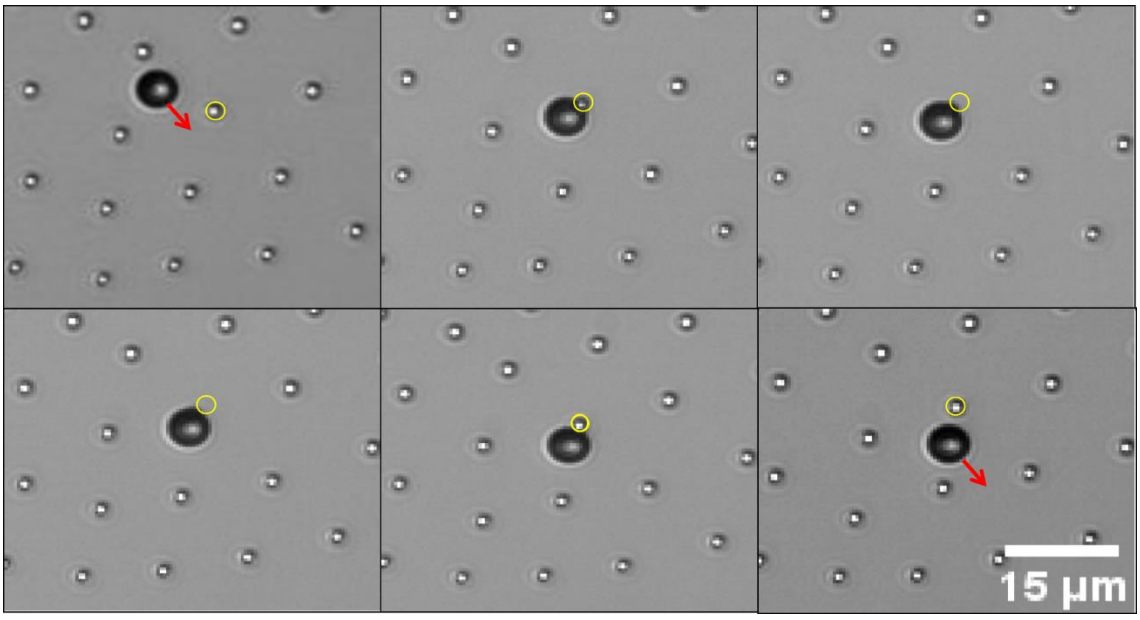

Figure 2.20: *The active particle moving through the lattice structure with the red arrow showing its direction of movement. The yellow circles shows the original position of the lattice particle being approached by the swimmer and how the lattice particles position is changed over time.*

The average velocity of the swimming particles was calculated when the swimmer is at a lattice particle and when it's swimming freely away from any lattice particles, shown in

Table 5. The average velocity of the particles does not change significantly when the swimmer is at the site of a lattice particle, proving that the interaction between the lattice particles and the active particles is not the cause of the increased velocity of the particles.

Table 5

Particle	Average Velocity of Swimmer at Lattice Particle (μm/s)	Average Velocity of Swimmer away from Lattice Particle (μm/s)
I	4.502	4.933
II	3.831	3.766
III	4.511	4.933
IV	4.547	4.661
Average	4.348	4.573

2.4.6 Particle Orientation at the Interface

By utilising the gel trapping technique described above we obtained SEM images of the particles in their interfacial orientation. The images in Figure 2.21 are taken through the "water phase" so the particles are oriented the opposite way up to the interface in the fluid cell. The white parts of the particles in the images are the polystyrene with the darker parts being the platinum coated regions of the particles. The particles which are fully white have the entire platinum region in the oil phase so therefore will not swim as the catalyst has no access to the fuel. The fully dark particles have the platinum section fully in the water phase and the particles with bright and dark areas are tilted at the interface. The swimming particles can take either of these orientations at the interface and have the ability to swim.

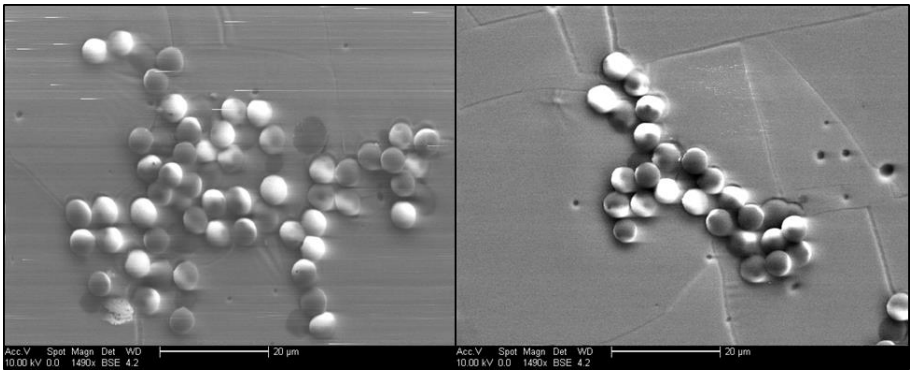

Figure 2.21: *SEM images of the active particle orientations at the oil-water interface. The brighter parts of the particle is the uncoated polystyrene side and the darker areas the platinum coated side. The particles which are fully white have the platinum side fully engulfed in the oil phase, the fully dark particles have the platinum fully in the water phase and other particles are tilted at the interface.*

The majority of the Janus particles take a tilted orientation at the interface with a section of the platinum face in the water phase and in the oil phase, with almost 60% of the particles in this

position. 25% of the particles have the platinum face completely in the oil phase and 16% of the particles sit with the platinum face completely in the water phase. As the particles with the platinum fully engulfed in the oil phase will not have an active motion, a further majority of the swimming particles will take a tilted orientation at the interface. This agrees well with results from literature in [25][26].

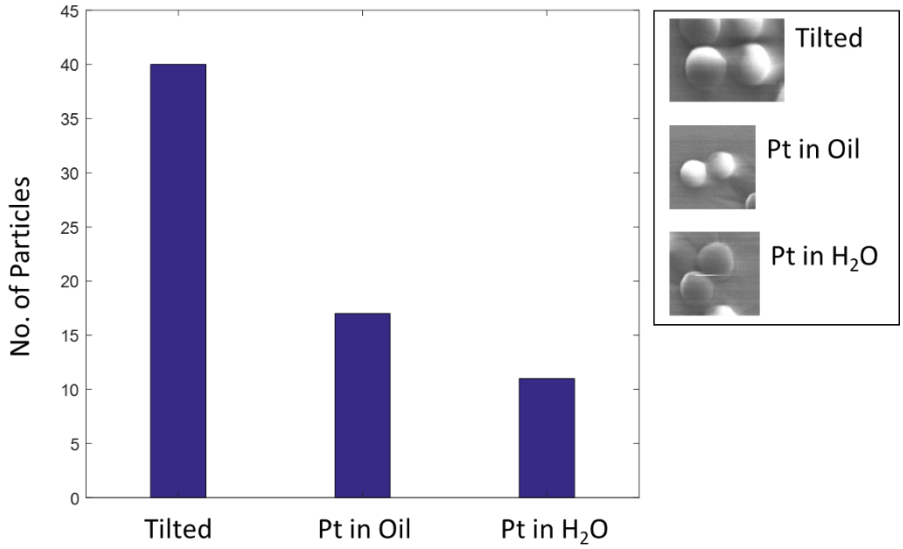

Figure 2.22: *Histogram of the particle orientation distribution. With the bars representing particles with a tilted orientation, particles with platinum surface fully in the oil phase and particles with platinum surface fully in the water phase. The majority of the particles sit at a tilted orientation.*

2.5 Conclusion and Outlook

In this project the motion of active particles at an oil-water interface was studied. Janus particles which showed a directed motion in hydrogen peroxide solutions were successfully synthesised. The movement of these particles was then tracked in bulk, at a bare oil-water interface and at an oil-water interface with a lattice of passive particles present.

The results show that the active particles swimming at a bare interface change direction frequently whereas when the swimmers are confined in a 2-dimensional lattice they take a more linear track. This steering of the particle allows for an increase in the mean squared displacement for the swimmers in the lattice and also an increased velocity.

The swimming particles seem to display an interesting catch and release mechanism of the lattice particles. Upon calculating the velocities of the swimming particles while touching a lattice particle and not touching one, we saw little change in the velocities. This shows that this seeming interaction between the active and inactive particles does not affect the velocity of the swimmer. From this we can say that it is most likely that the increase in velocity comes from the lower frequency in directional changes within a lattice.

The particles most likely sit in a tilted orientation at the interface. The particles could be pinned slightly below the interface due to the inherent roughness of the platinum coating. Further work needs to be done on this area as the particles should be separate at the interface and not clustered. By looking at clusters of particles we can get inaccurate results as the aggregation can cause the particles to change configurations.

A prospective application for this research could be cargo transport. Baraban *et al.* [32] showed that active Janus particles, similar to the ones utilised in this project, can be used for the transport of passive particles, shown in Figure 2.23. The active particles at the base of a glass cell show a directed motion in hydrogen peroxide and can then push passive particles of the same size to other areas of the cell. In order to achieve this the bonds between the passive particles at the interface need to be weakened, either by a decrease in surface coverage to remove dipolar repulsion or by addition of a salt to the oil phase. The active particles could then have the ability to capture the passive particles and move them along the interface.

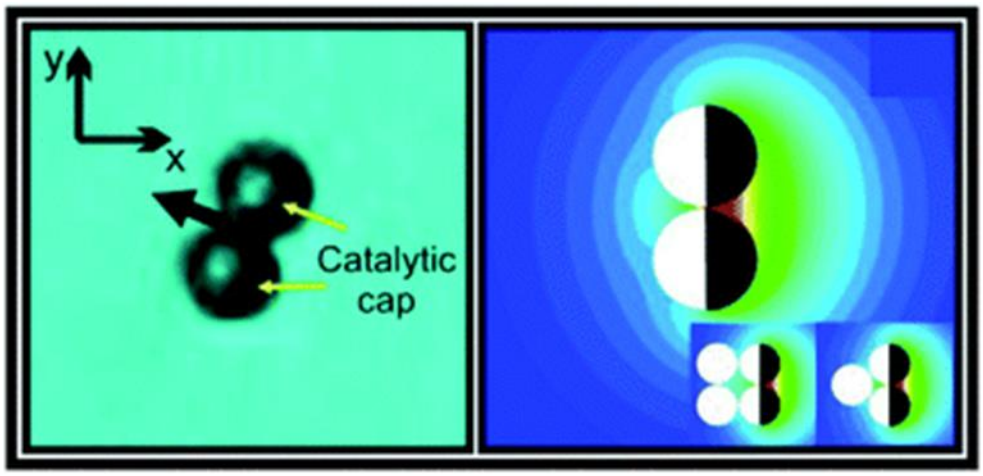

Figure 2.23: *Active Janus particles can be used as a method of transporting cargo. Active particles consisting of a polystyrene particles semi-coated in platinum can capture and push inactive particles through a hydrogen peroxide solution. From Figures 1 and 4 in [32].*

3 Acknowledgements

I would like to express my gratitude to everyone who contributed to this project and helped me along the way. Firstly, I would like to thank Fuqiang for his daily supervision and support throughout my time in FCC. I would also like to thank Willem for his supervision and enthusiasm about my project.

A huge thank you to: Daniël for providing particles used in this research; Pepijn for providing the tracking code; and Kanvaly and Hans Meeldijk for their help with SEM imaging. Everyone involved in the Friday Brainstorm sessions are also thanked for the helpful advice and comments.

Thank you to all other members of FCC and the master students in particular for creating such a nice working environment and helping to make my time here such a positive experience.

Finally I would like to thank my family and Sam for all the support (both emotional and financial) and encouragement through this whole process.

4 Bibliography

[1] S. U. Pickering, “72, 156,” pp. 2001–2021, 2001.

[2] B. P. Binks, “Particles as surfactants - Similarities and differences,” *Curr. Opin. Colloid Interface Sci.*, vol. 7, no. 1–2, pp. 21–41, 2002.

[3] J. C. Loudet, A. M. Alsayed, J. Zhang, and A. G. Yodh, “Capillary interactions between anisotropic colloidal particles,” *Phys. Rev. Lett.*, vol. 94, no. 1, pp. 2–5, 2005.

[4] B. Madivala, J. Fransaer, and J. Vermant, “Self-assembly and rheology of ellipsoidal particles at interfaces,” *Langmuir*, vol. 25, no. 5, pp. 2718–2728, 2009.

[5] S. Sacanna *et al.*, “Shaping colloids for self-assembly.,” *Nat. Commun.*, vol. 4, p. 1688, 2013.

[6] H. R. Sheu, M. S. El-Aasser, and J. W. Vanderhoff, “Uniform nonspherical latex particles as model interpenetrating polymer networks,” *J. Polym. Sci. Part A Polym. Chem.*, vol. 28, no. 3, pp. 653–667, 1990.

[7] R. Aelion, A. Loebel, and F. Eirich, “Hydrolysis of Ethyl Silicate,” *J. Am. Chem. Soc.*, vol. 72, no. 12, pp. 5705–5712, 1950.

[8] C. J. Morin, L. Geulin, A. Desbène, and P. L. Desbène, “Study of the acid hydrolysis of (3-methacryloxypropyl)trimethoxysilane by capillary electrophoresis-ion-trap mass spectrometry,” *J. Chromatogr. A*, vol. 1032, no. 1–2, pp. 327–334, 2004.

[9] S. Sacanna, W. T. M. Irvine, L. Rossi, and D. J. Pine, “Lock and key colloids through polymerization-induced buckling of monodisperse silicon oil droplets,” *Soft Matter*, vol. 7, no. 5, pp. 1631–1634, 2011.

[10] T. S. Horozov, R. Aveyard, J. H. Clint, and B. P. Binks, “Order - Disorder Transition in Monolayers of Modified Monodisperse Silica Particles at the Octane - Water Interface,” *Langmuir*, vol. 19, no. 7, pp. 2822–2829, 2003.

[11] T. S. Horozov, R. Aveyard, J. H. Clint, and B. P. Binks, “Order-disorder transition in monolayers of modified monodisperse silica particles at the octane-water interface,” *Langmuir*, vol. 19, no. 7, pp. 2822–2829, 2003.

[12] D. Stamou, C. Duschl, and D. Johannsmann, “Long-range attraction between colloidal spheres at the air-water interface: The consequence of an irregular meniscus,” *Phys. Rev. E - Stat. Physics, Plasmas, Fluids, Relat. Interdiscip. Top.*, vol. 62, no. 4 B, pp. 5263–5272, 2000.

[13] P. A. Kralchevsky and K. Nagayama, “Capillary interactions between particles bound to interfaces, liquid films and biomembranes,” *Adv. Colloid Interface Sci.*, vol. 85, no. 2, pp. 145–192, 2000.

[14] B. J. Park and E. M. Furst, “Attractive interactions between colloids at the oil–water interface,” *Soft Matter*, vol. 7, no. 17, p. 7676, 2011.

[15] R. Van Hooghten, L. Imperiali, V. Boeckx, R. Sharma, and J. Vermant, "Rough nanoparticles at the oil–water interfaces: their structure, rheology and applications," *Soft Matter*, vol. 9, no. 45, p. 10791, 2013.

[16] S. Reynaert, P. Moldenaers, and J. Vermant, "Control over colloidal aggregation in monolayers of latex particles at the oil-water interface," *Langmuir*, vol. 22, no. 11, pp. 4936–4945, 2006.

[17] S. J. Ebbens, "Active colloids: Progress and challenges towards realising autonomous applications," *Curr. Opin. Colloid Interface Sci.*, vol. 21, pp. 14–23, 2016.

[18] J. Zhang, X. Zheng, H. Cui, and Z. Silber-Li, "The self-propulsion of the spherical Pt-SiO2 Janus micro-motor," *Micromachines*, vol. 8, no. 4, pp. 1–17, 2017.

[19] M. Assenheimer and V. Steinberg, "Critical phenomena in hydrodynamics," *Eur. News*, p. 143, 1996.

[20] J. Palacci, S. Sacanna, S. Kim, G. Yi, D. J. Pine, and P. M. Chaikin, "colloids," 2014.

[21] J. Zhang, B. A. Grzybowski, and S. Granick, "Janus Particle Synthesis, Assembly, and Application," *Langmuir*, vol. 33, no. 28, pp. 6964–6977, 2017.

[22] W. Wang, W. Duan, S. Ahmed, T. E. Mallouk, and A. Sen, "Small power: Autonomous nano- and micromotors propelled by self-generated gradients," *Nano Today*, vol. 8, no. 5, pp. 531–534, 2013.

[23] J. R. Howse, R. A. L. Jones, A. J. Ryan, T. Gough, R. Vafabakhsh, and R. Golestanian, "Self-Motile Colloidal Particles: From Directed Propulsion to Random Walk," *Phys. Rev. Lett.*, vol. 99, no. 4, pp. 8–11, 2007.

[24] H. Ke, S. Ye, R. L. Carroll, and K. Showalter, "Motion Analysis of Self-Propelled Pt- Silica Particles in Hydrogen Peroxide Solutions," *J. Phys. Chem. A*, vol. 114, no. 17, pp. 5462–5467, 2010.

[25] X. Wang, M. In, C. Blanc, M. Nobili, and A. Stocco, "Enhanced active motion of Janus colloids at the water surface," *Soft Matter*, vol. 11, no. 37, pp. 7376–7384, 2015.

[26] B. J. Park, T. Brugarolas, and D. Lee, "Janus particles at an oil–water interface," *Soft Matter*, vol. 7, no. 14, p. 6413, 2011.

[27] V. N. Paunov, "Novel method for determining the three-phase contact angle of colloid particles adsorbed at air-water and oil-water interfaces," *Langmuir*, vol. 19, no. 19, pp. 7970–7976, 2003.

[28] R. Aveyard, J. H. Clint, D. Nees, and V. N. Paunov, "Compression and structure of monolayers of charged latex particles at air/water and octane/water interfaces," *Langmuir*, vol. 16, no. 4, pp. 1969–1979, 2000.

[29] P. Pieranski, “Two-dimensional interfacial colloidal crystals,” *Phys. Rev. Lett.*, vol. 45, no. 7, pp. 569–572, 1980.

[30] W. Chen, S. Tan, Z. Huang, T. K. Ng, W. T. Ford, and P. Tong, “Measured long-ranged attractive interaction between charged polystyrene latex spheres at a water-air interface,” *Phys. Rev. E - Stat. Nonlinear, Soft Matter Phys.*, vol. 74, no. 2, pp. 1–14, 2006.

[31] C. L. Wirth, E. M. Furst, and J. Vermant, “Weak Electrolyte Dependence in the Repulsion of Colloids at an Oil–Water Interface,” *Langmuir*, vol. 30, no. 10, pp. 2670–2675, 2014.

[32] L. Baraban, M. Tasinkevych, M. N. Popescu, S. Sanchez, S. Dietrich, and O. G. Schmidt, “Transport of cargo by catalytic Janus micro-motors,” *Soft Matter*, vol. 8, no. 1, pp. 48–52, 2012.

5 Appendices

5.1 MATLAB Codes

This is the MATLAB code used to find the particles position in each frame. This code was obtained from Pepijn Moerman. Some explanations for the steps are given in green and shown with "%".

```
obj=find_pos(obj,initialize)
        %Creates obj.pos by tracking particles
        %Function is interactive and requires human input
        %initialize indicates whether or not existing parameters are
        %used for particle_finding or a new set is generated
        %interactively. Use existing set is (0), generate new set
        %interactively is (1). Default is (1)
        if nargin<2
           initialize=1;
        end
        if isempty(obj.posparam)
           initialize=1;
        end
        MSGID3='MATLAB:imagesci:tifftagsread:expectedTagDataFormatMultiple';
        warning('off', MSGID3)
        fname=[obj.foldername obj.filename '.tif'];
        if initialize==1
           output=particlefinder_class(fname);
        else
           output=particlefinder_class(fname,obj.posparam);
        end
        obj.pos=output{1};
        obj.posparam=output{2};

    end
    function pos=get_positions(obj)
       %Gets the positions from object
       pos=obj.pos;
    end
    function obj=change_scale(obj,scale_temp)
       %Manually change the scale
       obj.scale=scale_temp;
    end
    function obj=change_framerate(obj,framerate_temp)
       %Manually change the framerate
       obj.framerate=framerate_temp;
    end
```

Shown here is the MATLAB code for tracking the position of the particles.

```
function obj=track_obj(obj,initialize)
        %Takes obj and tracks the particle positions
        %outputs a n x 4 matrix organized as [x y f ID]
        %Initialize indicates whether or not to use existing parameters
```

```
    %for tracking or define new ones. Use existing ones is (0) and
    %define new ones is (1). Default is (1).
    if nargin<2
       initialize=1;
    end
    if isempty(obj.trparam)
       initialize=1;
    end

    if isempty(obj.pos)
       obj=find_pos(obj);
    end

    if initialize==1
       % Set parameters for trackingsoftware
       maxdisp=get_numerical_input('What is the max displacement? ');
       param.mem=get_numerical_input('How long can a particle go missing? ');
       param.dim=2; % dimensionality of data
       param.good=get_numerical_input('What is the minimal number of frames for a track to be accepted? ');
       param.quiet=1; % 0 = text, 1 = no text
    else
       maxdisp=obj.trparam{2};
       param=obj.trparam{1};
    end

    moveon=1;
    try trace=track(obj.pos,maxdisp,param);
    catch
       disp('Tracking failed. Try using different parameters');
       moveon=0;
    end
    if moveon==1
       obj.NOP=max(trace(:,4));
       obj.NOF=max(trace(:,3));
       obj.tr=trace;
       obj.trparam={};
       obj.trparam{1}=param;
       obj.trparam{2}=maxdisp;
       obj=complete_trace(obj);
    end
```

This is the code used for calculating the MSD of each particle.

```
obj=calc_MSD(obj,fraction)
    %calculates mean squared displacement per particle and the
    %average mean squared displacement.
    %fraction indicated what fraction of the trajectory to use to
    %calculated MSD (last few steps have poor statistics). Default
    %is 1/3; i.e. fraction is 3;

    if nargin<2
       fraction=3;
    end
```

```
  if isempty(obj.tr)
    obj=track_obj(obj);
  end
  trace=obj.tr;
  nparts=obj.NOP;
  nframes=obj.NOF;
  framerate_temp=obj.framerate;
  scale_temp=obj.scale;
  obj.MSD=cell(nparts+1,2);

  if length(trace(:,1))~=max(trace(:,4))*max(trace(:,3))
    obj=complete_trace(obj);
  end

  MSD_tot=NaN(floor(nframes/fraction),nparts);
  for i=1:nparts
    % Select the part of the file about particle i
    trj = trace((i-1)*nframes+1:i*nframes,1:3);
    if ~isempty(trj)

      % Find thelength of the trajectory of particle i
      tmax=length(trj(:,1));

      % Define empty matrix for MSD
      MSD_temp=NaN(floor(tmax/fraction),nparts);

      % For a time interval of 1 to 1/3 of the length of the trajectory
      for t=1:floor(tmax/fraction)
        MSD_all=[];
        %Create two matrixes with a difference t between them
        a_frontstep=trj(t:length(trj),1:2);
        a_backstep=trj(1:length(trj)-t+1,1:2);
        %Substract to obtain MSD
        MSD_all=(a_frontstep(:,1)-a_backstep(:,1)).^2+(a_frontstep(:,2)-a_backstep(:,2)).^2;
        MSD_all=MSD_all(~isnan(MSD_all));
        %Average to obtain average MSD for t and save
        MSD_temp(t,1)=t/framerate_temp;
        MSD_temp(t,2)=mean(MSD_all(:,1))*scale_temp;
      end

      %End if statements if matrix is empty after removing stuck particles
    end
    %End loop over particle number
    obj.MSD{1+i,1}=i;
    obj.MSD{1+i,2}=MSD_temp(:,1:2);
    MSD_tot(:,i)=MSD_temp(:,2);
  end
  obj.MSD{1,1}='Average';
  obj.MSD{1,2}=[MSD_temp(:,1) mean(MSD_tot(:,:),2)];

end
```

5.2 Error in Mean Squared Displacement

The separate plots for the MSD of the active particles at the oil-water interface have big differences so the errors are shown in Figure 5.1. The particles swimming with no lattice have a standard error of 16.7931 and the particles swimming within a lattice have a standard error of 21.7159.

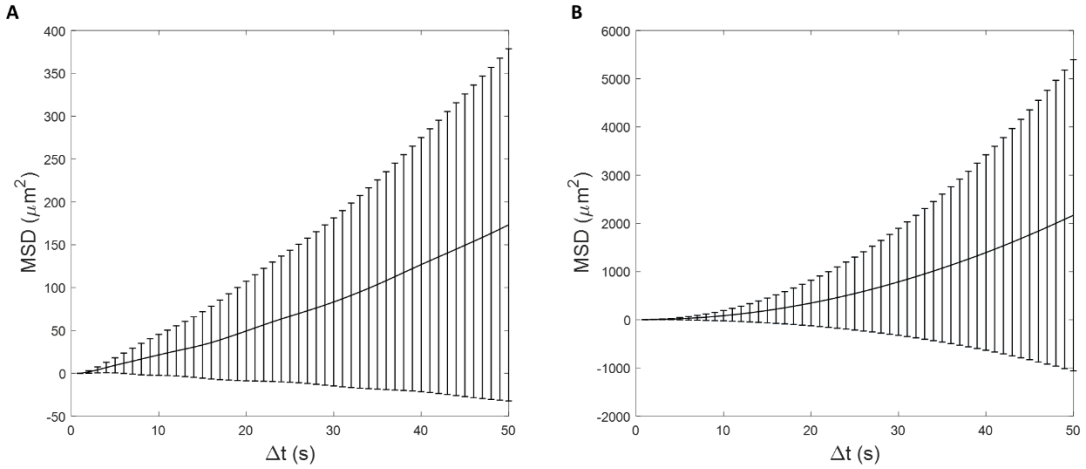

Figure 5.1: *A: The error for MSD of active particles at the interface with no lattice. B: The error for MSD of active particles at the interface within lattice structure.*